Dynamics Technology, Inc.

DT-8178-02

TURBULENCE MEASUREMENTS IN A SWIRLING CONFINED JET FLOWFIELD USING A TRIPLE HOT-WIRE PROBE

November, 1982

By: S.I. Janjua and D.K. McLaughlin

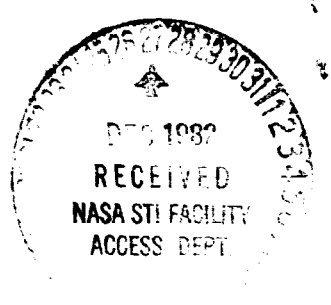

Dynamics Technology, Inc.
22939 Hawthorne Blvd., Suite 200
Torrance, California 90505
(213) 373-0666

This report has undergone an extensive internal review before release, both for technical and non-technical content, by the Division Manager and an independent internal review committee.

Division Manager:

Internal Review:

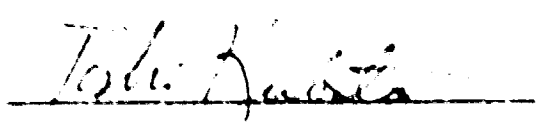

FOREWORD

This document reports on the turbulence measurements performed in a swirling, confined jet flowfield. The experiments were supported by Oklahoma State University (Purchase Requisition 31256) as part of NASA Grant No. NAG 3-74, "Investigations of Flowfields Found in Typical Combustor Geometries." The experiments conducted in the Dynamics Technology facility were performed with a triple hot-wire probe utilizing a specially constructed probe drive fabricated by students at Oklahoma State University. Included as Appendix A of this report is AIAA paper No. 82-1262 which reports on turbulence measurements performed in a confined jet at Oklahoma State using a six-orientation single hot-wire technique. A portion of the analysis of the data in that paper was performed at Dynamics Technology under the noted subcontract.

The authors would like to acknowledge the assistance of Professor David Lilley of OSU and especially his students in support of our experiments. The financial support of NASA Lewis Research Center and the Air Force Wright Aeronautical Laboratories is also acknowledged. Finally the authors would like to thank Professor Toshi Kubota and Dr. Robert Gran for their suggestions regarding the interpretation of the experimental data.

ABSTRACT

The investigation of an axisymmetric swirling confined jet flowfield, similar to the ones encountered in gas turbine combustors, has been carried out using a triple hot-wire probe. The raw data from the three sensors are digitized using ADC's and stored on a Tektronix 4051 computer. The data are further reduced on the computer to obtain time-series for the three instantaneous velocity components in the flowfield. Finally, the time-mean velocities and the turbulence quantities are deduced.

Qualification experiments were performed and where possible comparisons are made with the results of independent measurements. For example, the mean velocity components are compared with the results of five-hole pitot probe measurements. The major qualification experiments involved measurements performed in a non-swirling flow compared with conventional X-wire measurements. In the swirling flowfield advantages of the triple wire technique over the previously used multi-position single hot-wire method are noted. The results of the present measurements provide a data base with which the predictions of turbulence models in a recirculating swirling flowfield can be evaluated in detail.

TABLE OF CONTENTS

NOMENCLATURE

A,B,C	Calibration constants in Equation (3.1)
D	Test section diameter
d	Inlet nozzle diameter
E	Hot-wire voltage
u_n	Velocity normal to a single wire
$\tilde{u},\tilde{v},\tilde{w}$	Velocity components in the coordinate system defined by a single wire.
u_o,v_o,w_o	Velocity components in the coordinate system defined by the three wires.
u',v',w'	Velocity components in the coordinate system defined by the probe support axis.
u	Instantaneous axial velocity in facility coordinate system.
v	Instantaneous radial velocity in facility coordinate system.
w	Instantaneous swirl velocity in facility coordinate system
G	Pitch factor.
K	Yaw factor
N	Number of points digitized per channel
r	Radial location in the flowfield.
x	Axial location in the flowfield.
z	Effective cooling velocity acting on a wire.
α	Side-wall expansion angle.
ϕ	Swirl vane angle.
θ_1	Probe pitch angle.
θ_2	Probe yaw angle.

Subscripts

$1,2,3$	Refer to the three wires of a triple-wire probe.
rms	Root-mean-squared quantity.

Superscripts

$\overline{(\quad)}$	Time-mean averaged quantity.
$(\ ')$	Fluctuating quantity.

1. INTRODUCTION

1.1 Background and Previous Studies

Swirling confined jets have been under intensive investigation in the recent years. One application of such flowfields is a gas turbine combustor, an example of which is shown in Figure 1. Flowfields within such combustors typically have a rapid expansion and strong swirl imparted to the incoming air, which result in corner and central recirculation zones. The presence of swirl and the re-circulation zones increase the complexity in terms of fluid dynamic analyses of such flowfields. This complexity is further increased by the processes of combustion and heat transfer within the flowfield. Despite the complexity of combustor flows, significant progress is being made in their analysis as discussed in Reference 1.

During an initial attempt to perform measurements of mean velocity and turbulence quantities, a much simplified combustor flowfield was modeled. Figure 2 shows the schematic of idealized geometry with a control of side wall expansion and degree of swirl imparted to the flow. The figure shows various recirculation regions experienced in such a flowfield. This idealized swirling confined jet is being investigated at Oklahoma State University and at Dynamics Technology, with a variety of methods of approach. Analytically, a computer code (STARPIC) presents a theoretical model designed specifically to calculate the swirling confined jet flowfields [2]. Experimentally, a series of flow visualization experiments coupled with 5-hole pitot probe measurements have been used to characterize the time-mean flowfield[3].

In addition to the mean properties, turbulence measurements are being performed using various hot-wire techniques. At Oklahoma State University, a technique of using a single, normal hot-wire at six different orientations has been developed which can measure time-mean velocities and normal and shear stresses. Some of the analysis of the measurements was performed at Dynamics Technology under the present sub-contract and is therefore included here as Appendix A.

The six-orientation technique is basically a statistical technique applicable to stationary turbulent flows which uses mean voltage and root-mean-square voltage fluctuation measurements and an extensive data reduction method to produce estimates of the components of mean velocity together with normal and shear turbulent stresses.

1.2 Present Study

At Dynamics Technology, a triple-wire measurement technique has been developed for the purpose of measuring mean velocity and turbulent stresses. The three wires are simultaneously operated by three closely matched constant temperature anemometers, from which time series of these velocity components can be deduced. The instantaneous signals are digitized using ADC's which are controlled by a Tektronix 4051 computer. The subsequent data analysis is performed by digitally correlating the three signals and thereby obtaining the time-mean velocities and the velocity fluctuation products which can be averaged to produce Reynolds stress estimates. A significant advantage of the three-wire method is that the data reduction is performed on instantaneous measurements so that time records of velocity components (and fluctuations) can be obtained. Consequently more detailed information on the turbulence (including time domain information) can be obtained which is not possible with the single wire, six-position technique.

The data analysis is based on a study done by Yavuzkurt, Crawford and Moffat [5] who used a triple-wire probe in a three dimensional turbulent flowfield. Yavuzkurt et al. developed a network of analog devices with which to process their signals. This data processing in the present study has been replaced by software coding operating on digitized signals.

2. PROBE DESCRIPTION AND INSTRUMENTATION

2.1 The Triple-Wire

The three-wire probe used in the present study is DISA type 55F81. (See Figure 3.). The three sensors are 5 μm diameter platinum plated tungsten wires. The wires are oriented in a mutually orthogonal array. The probe support lies symmetrically between the three wires making an angle of 54.7 degrees with each of the wires or 35.3 degrees with the plane defined by any of the two wires (see Figure 4). The gold-plated and stainless-steel prongs are embedded in three independent ceramic bodies mounted in the stainless-steel probe shank.

The probe is operated by three separate but closely matched constant temperature anemometers (DISA type 55C12). The hot-wire raw signals are conditioned by DISA type 55N20 signal conditioners. The signal conditioners allow low pass filtering of the hot-wire signals at a desired frequency.

2.2 Experimental Facility

Figure 5 shows the overall schematic of the entire facility. It consists of a 1400 C.F.M. fan manufactured by Joy Manufacturing Co. The fan drives the air through a 9" diameter section of flow straighteners into a diffuser which has two perforated plates inside in order to prevent flow separation within the diffuser. The flow then passes through a turbulence management section which has several screens and flow straighteners to decrease the turbulence levels. The air then enters a contraction section

and exits through a round jet of 6 inch diameter and expands into the test section which consists of a five foot long plexiglass tube 12 inches in diameter. A swirler designed and built at Oklahoma State University can be installed at the nozzle exit along with the desired expansion block (see Figure 5.).

2.3 The Probe Drive

The probe drive, shown in Figure 6 was designed specifically for triple-wire measurements. The drive has three degrees of freedom: pitch and yaw, (necessary to aim the probe in the direction of the mean flow at any location in the flowfield) and vertical translation for surveying an axial station.

2.4 Data Acquisition System

The hot-wire signals from the three wires are digitized using analog-to digital converters which can scan each of the three channels simultaneously up to a sampling rate of 9 kHz. The ADC's are controlled by the Tektronix 4051 laboratory computer. The digitized data are stored on magnetic tape and further reduced and plotted using the laboratory computer. The entire data acquisition and reduction system is automated, thereby eliminating the intermediate handling of experimental data.

3. THEORY AND DATA REDUCTION

3.1 Response Equations

Before measurements in a turbulent flowfield, the triple-wire probe is calibrated in the uniform-flow region of the free jet. A calibration equation relating velocity to the hot-wire voltage for a single wire can be written as:

$$E^2 = A + B\,U_n^{1/2} + C\,U_n \tag{3.1}$$

where E is the hot-wire voltage and U_n is the component of velocity normal to the wire. For a triple-wire, three such calibrations are required for the three individual sensors. There are two methods of calibration reported in literature. One method, used by Gaulier [6] for example, calls for orientation of the individual sensors normal to the calibration (in smooth potential flow) jet and thus obtaining an E vs U_n curve fit given in Equation (3.1). The second method, used by Yavuzkurt et al. [5], calls for orientation of the probe axis colinear with the calibration jet and resolving the velocity components in directions normal to the three wires to obtain an E vs U_n calibration for the three respective wires. For the present study, both the methods were tried and the method where the probe support axis is colinear with the jet was found to produce better results and hence is used in the analysis. Equation (3.1) can be now inverted and can be written in terms of the individual cooling velocities experienced by the three wires as:

$$Un_1 = \{ -B_1 + \{B_1^2 - 4C_1(A_1 - E_1^2)\}^{1/2}/2C_1\}^2$$

$$Un_2 = \{-B_2 + \{B_2^2 - 4C_2(A_1 - E_2^2)\}^{1/2}/2C_2\}^2 \tag{3.2}$$

$$Un_3 = \{-B_3 + \{B_3^2 - 4C_3(A_3 - E_3^2)\}^{1/2}/2C_3\}^2$$

Jorgensen[7] introduced the sensitivity of a normal single hot-wire to flow-field angularity by an equation:

$$z^2 = \tilde{v}^2 + G^2\,\tilde{u}^2 + K^2\,\tilde{w}^2 \tag{3.3}$$

where $\tilde{u},\tilde{v}$, and $\tilde{w}$ are velocity components in the coordinate system defined by the probe (see Figure 7), z is the apparent cooling velocity and the pitch and yaw sensitivity factors are defined by Jorgensen [7] as:

$$G = \frac{\tilde{v}\ (\tilde{u},\tilde{w} = 0)}{\tilde{u}\ (\tilde{v},\tilde{w} = 0)}$$

and

$$K = \frac{\tilde{v}\ (\tilde{u},\tilde{w} = 0)}{\tilde{w}\ (\tilde{u},\tilde{v} = 0)} \qquad (3.4)$$

evaluated from calibrations performed in the three directions defined by Figure 7. The apparent cooling velocity z_i is the velocity that would be calculated from the hot-wire voltage E_i (for the i^{th} wire) from one of equations (3.2).

As described in section 2, the wires of a triple-wire probe form a trihedral. Figure 8 shows the coordinate system (x_o,y_o,z_o) defined by the three wires. Equations (3.3) can now be written for each wire as:

$$\begin{aligned} z_1^2 &= K_1^2\, u_o^2 + V^2{}_o + G_1^2\, w_o^2 \\ z_2^2 &= G_2^2\, u_o^2 + K_2^2\, v_o^2 + w_o^2 \\ z_3^2 &= u_o^2 + G_3^2\, v_o^2 + K_3^2\, w_o^2 \end{aligned} \qquad (3.5)$$

Equation (3.5) can also be written in the matrix form as:

$$\begin{bmatrix} z_1^2 \\ z_2^2 \\ z_3^2 \end{bmatrix} = \begin{bmatrix} K_1^2 & 1 & G_1^2 \\ G_2^2 & K_2^2 & 1 \\ 1 & G_3^2 & K_3^2 \end{bmatrix} \begin{bmatrix} u_o^2 \\ v_o^2 \\ w_o^2 \end{bmatrix} \tag{3.6}$$

we can define a sensitivity matrix K given by:

$$K = \begin{bmatrix} K_1^2 & 1 & G_1^2 \\ G_2^2 & K_2^2 & 1 \\ 1 & G_3^2 & K_3^2 \end{bmatrix} \tag{3.7}$$

Equation (3.5) can be inverted to obtain velocity components in the x_o,y_o and z_o directions (coincident with the orientation of the three wires):

$$\begin{bmatrix} u_o^2 \\ v_o^2 \\ w_o^2 \end{bmatrix} = K^{-1} \begin{bmatrix} z_1^2 \\ z_2^2 \\ z_3^2 \end{bmatrix} \tag{3.8}$$

In calculating the velocity components u_o,v_o and w_o from three squared values it is assumed that each component is the positive square root of the squared quantity. This is equivalent to assuming that the velocity vector lies within 54.7 degrees of the probe axis. In highly turbulent regions, points in time in which the velocity is outside the 54.7 degree cone are incorrectly resolved. This is perhaps the most serious source of error in the triple-wire measurement technique.

In the calculation of the u_o,v_o and w_o velocity components at some points in time negative values of squared quantities are obtained (indicating

imaginary velocity components). We believe this is related to the situation in which the direction of the velocity vector is outside the 54.7 degrees probe cone. There are two ways in which we handle such data. The first method is to completely discard the point from the data set. The second method is to set the individual velocity component (whose squared value is negative) to zero and include the data point in the set. Comparison of final flowfield estimates calculated by the two ways provides a measure of the uncertainly of the quantity.

Using the above described methods, the u_o, v_o and w_o velocity components are calculated at each point in time. These data can then be transformed into a coordinate frame x',y' and z' defined by the probe support as shown in Figure 4 by:

$$\begin{bmatrix} u' \\ v' \\ w' \end{bmatrix} = \begin{bmatrix} \cos45\ \cos35 & \cos45\ \cos35 & \cos45\ \cos35 \\ -\cos45 & \cos45 & 0 \\ \cos45\ \sin35 & \cos45\ \sin35 & -\cos35 \end{bmatrix} \begin{bmatrix} u_o \\ v_o \\ w_o \end{bmatrix} \quad (3.9)$$

There is yet a final transformation that is performed to obtain the velocity components in the facility coordinates (x,y,z). This transformation depends upon the orientation of probe axis in the flow. Assuming θ_1 , to be the pitch angle and θ_2 be the yaw angle of the probe the final transformation equation can be written as:

$$\begin{bmatrix} u \\ w \\ v \end{bmatrix} = \begin{bmatrix} \cos\theta_1\ \cos\theta_2 & -\sin\theta_2 & -\cos\theta_2\ \sin\theta_1 \\ \cos\theta_1\ \sin\theta_2 & \cos\theta_2 & -\sin\theta_1\ \sin\theta_2 \\ \sin\theta_1 & 0 & \cos\theta_2\ \cos\theta_1 \end{bmatrix} \begin{bmatrix} u' \\ v' \\ w' \end{bmatrix} \quad (3.10)$$

where u is the instantaneous axial velocity, w is instantaneous swirl velocity and v is the instantaneous radial velocity. Thus Equation (3.10) gives the time series for the three velocity components u,v, and w in the facility coordinate system x,y and z.

Thus the time mean velocities are computed with

$$\bar{u} = \sum_{i=1}^{n} u_i/N$$

$$\bar{v} = \sum_{i=1}^{N} v_i/N \qquad (3.11)$$

$$\bar{w} = \sum_{i=1}^{N} w_i/N$$

where N is the total number of points digitized per channel.

Similarly, the turbulent normal stresses can be written as:

$$\overline{u'^2} = \frac{\sum_{i=1}^{N} (u_i - \bar{u})^2}{N}$$

$$\overline{v'^2} = \frac{\sum_{i=1}^{N} (v_i - \bar{v})^2}{N} \qquad (3.12)$$

$$\overline{w'^2} = \frac{\sum_{i=1}^{N} (w_i - \bar{w})^2}{N}$$

Finally, the turbulent shear stresses can be written as

$$\overline{u'v'} = \frac{\sum_{i=1}^{N} (u_i - \bar{u})(v_i - \bar{v})}{N}$$

$$\overline{u'w'} = \frac{\sum_{i=1}^{N} (u_i - \bar{u})(w_i - \bar{w})}{N} \qquad (3.13)$$

$$\overline{v'w'} = \frac{\sum_{i=1}^{N} (v_i - \bar{v})(w_i - \bar{w})}{N}$$

Equation (3.2) through (3.13) are solved on a Tektronix 4051 computer using the digitized raw signals from the three wires. The computer is equipped with a graphics package which facilitates the plotting of radial and axial distributions of time-mean and turbulence quantities. These data are presented in the next section.

4. RESULTS

Measurements of time-mean and turbulence quantities using a triple-wire probe were carried out in the idealized, non-reactive flowfield at various axial locations. Experiments were performed with the swirler vane angle set at 38 degrees and the side wall expansion angle α of 90 degree.

4.1 Data Sampling and Reduction:

As discussed earlier the signals from the three wires sometimes experience large differences generating negative values for squared quantities in

Equation 3.8. We suspect the problem to be caused by large local flowfield angles. Another possibility is that the turbulent scale sizes in the thin shear layer portions of the flowfield are small, and in some cases of comparable size to the triple hot-wire probe. In these cases probe resolution problems could lead to inaccuracies such as those experienced in the data.

As discussed earlier data are either discarded or processed by setting individual unresolvable velocity components to zero.The effect of discarding data is difficult to estimate. Initially, a large number of data points are recorded so that enough points are retained to maintain statistical significance. This is tested by comparing the results of processing 100, 200 and 400 data points and demonstrating "convergence" of the time-mean estimates. A second method involved comparing data calculated from the two methods of handling data with negative square roots discussed above. The most reliable method for estimating the accuracy of the data processing technique however, involved comparing results of the three-wire measurements with the results of independent measurements. In the swirling flowfields comparisons are made with measurements of mean velocity components made with a five-hole pitot probe. In non-swirling flowfields comparisons are made with conventional x-wire measurements performed by Chaturvedi [9] of both mean and turbulent velocity components. Finally, comparisons are also made with turbulence measurements performed in an identical swirling confined jet flowfield [4] using a six-orientation, single hot-wire technique. However, it appears that the present three-wire probe technique is in fact more accurate and reliable than the six-orientation, single wire method. This will be discussed further with the presentation of the measurement results.

4.2 Technique Verification in Non-Swirling Flow:

Preliminary measurements were performed in a non-swirling confined jet at x/D = 2.0 with ϕ = 0 and α = 90 degrees. The results are compared with a similar study performed by Chaturvedi[9] in a corresponding flow situation using a cross-wire probe. Figure 9 shows the radial distribution of time-mean and turbulence quantities. The two studies show very favorable agreement. Overall, the results show improvement over the results obtained by the six-orientation hot-wire technique reported in Reference 4, Appendix A. In particular, the radial turbulence intensity, when measured by the six-orientation technique was lower than the one measured by Chaturvedi[9] (at the x/D=2 station; see Reference 4). The triple-wire measurements show the radial turbulence intensity to agree very well with the Chaturvedi measurements. Generally speaking, the non-swirling confined jet measurements verify the triple-wire technique.

4.3 Mean-Velocity Field in Swirling Flow:

In a swirling confined jet flowfield, the axial and azimuthal velocity components are the two dominating components. The swirling confined jet flowfield measurements reported here have all been performed with parameters D/d=2, the swirl angle Φ=38 deg and the expansion angle α=90 deg. These parameters all correspond exactly to those used by Yoon[8] in an experimental study of the mean flow of the confined swirling jet. Yoon's measurements were all performed with a five-hole pitot probe at axial coordinates x/D=0.5,1.0,1.5, etc. In addition, he reported radial distributions of mean axial and swirl velocity components in the confined jet exit plane (at x/D=0). These velocity measurements indicate that the central recirculation zone starts at the base of the center hub. Outside of the center hub wake, the angle of the flow is approximately 28 deg. to the facility axis (compared with the blade angle ϕ of 38 deg). Figure 10, 11 and 12 show the radial profiles of the axial, radial, and azimuthal components of mean velocity. The data are compared with the five-hole pitot

probe measurements[3]. The two studies are in excellent agreement in the case of the axial component of mean velocity. The radial component of mean velocity also shows favorable agreement with the five hole pitot probe measurements for x/D 21. The swirl component measured by the triple-wire however, is up to twenty five percent lowe. than the one measured by the five- hole pitot probe at axial location of 1.5 and higher. At lower axial locations, the two measurements seem to agree very well.

As mentioned earlier, the measurements have been performed in a swirling confined jet in which the angles of the swirl blades have been set to 38°. After expanding to the larger diameter (D=30 cm) from the exit diameter (D=15 cm), local flow angles significantly increase to near 60° to the facility axis. The differences in the swirl velocity component measurements, seen in Figure 12, represent differences in local flowfield angles of up to 10°. The reason for this discrepancy is not known at this time. It is important to note however, that measurements of the swirl velocity component made with both the present three-wire method, and with the six-orientation single-wire technique are in almost perfect agreement (Compare solid symbols in Figure 12 with solid symbols in Figure 10, Appendix A).

4.4 Turbulence Intensity Measurements:

The primary purpose of the hot-wire probe is to measure the velocity fluctuations in a flowfield, taking advantage of the inherent fast time response of the instrument. A triple-wire probe makes it possible to measure the three components of the turbulence velocity in the swirling flow under investigation. Figures 13, 14 and 15 shows the radial distributions of the mean-square of three components of the turbulence velocity. The triple-wire data are compared with data obtained with the six-orientation hot-wire technique[4]. The two studies show reasonable agreement in quantifying the mean square of three components of the turbulence velocity.

In general the turbulent fluctuations are higher in regions of higher mean shear, such as evidenced on the edge of the recirculation region at an axial station x/D=0.5. However, there appear to be substantial turbulence levels throughout the recirculation region which we suspect is caused by the large scale "breathing" of the region. Understanding of the phenomenon will require more detailed measurements and signal analysis than was possible in this study.

4.5 Turbulent Shear Stresses:

Shear stresses are the most difficult turbulent quantities to measure accurately in a complex three-dimensional flowfield. Uncertainities in measurements of mean velocities and turbulence intensities are multiplied in determination of the shear stresses. Figures 16, 17 and 18 show the turbulent shear stresses deduced from the three-wire hot-wire measurements. When compared with the corresponding measurements performed in the non-swirling confined jet, (Figure 9), it can be seen that at most axial stations the radial location of highest turbulent shear stresses has moved outwards, corresponding to the shear layer displacement induced by the centrifugal forces. Note, that the measurements produce primarily negative values of the shear stress component $\overline{u'v'}$ which is expected in the viscinity of the recirculation region where the gradient of the axial velocity ($\partial\bar{u}/\partial r$) is predominantly positive.

4.6 Comparison of the Three-Wire and the Six-Orientation Single Hot-Wire Measurement Techniques:

The three-wire measurement technique was adopted to the present research study with the idea that improved experimental data would result. In particular, accurate estimates of turbulent shear stresses are difficult to obtain with any measurement technique (laser Doppler and hot-wire anemometry being the two most practical). Measurements were previously performed in the Oklahoma State University confined jet facility (with

α=90 deg and ϕ=38 deg) with the six-orientation single hot-wire technique. The resulting data are shown on many of the present figures and in more complete form in Reference 4 included as Appendix A.

The $\overline{u'v'}$ data deduced from the six-orientation single hot-wire measurements are all shown as positive because the method used in that study was unable to distinguish between positive and negative radial velocity components. If the six-orientation single-wire data were assigned their expected sign (to correspond to the results of the three-wire measurements) then the two sets of data would be in closer agreement. However, the $\overline{u'v'}$ data from the six-orientation single wire technique are usually larger in magnitude than the triple-wire data and exhibit significantly more scatter.

It could be argued that the $\overline{u'v'}$ data from the present method are more accurate than the single wire measurements. First, the time mean radial and axial velocity components are more accurately determined (as shown by the comparison with the 5 hole pitot probe measurements). Second, the turbulence measurements made in the non-swirling flow are slightly more accurate (as shown by comparison with Chaturvedi's x-wire measurements[9]). Finally, the magnitudes of all the turbulent stresses, as determined by the three-wire method, are of similar magnitude to the corresponding data measured in the non-swirling flow, if account is taken of the large changes in the recirculation geometry. The six-orientation single wire measurements indicate a larger $\overline{u'v'}$ component of the turbulent stress in comparison with the non-swirling confined jet. This does not seem reasonable to us because we would expect the centrifugal field to stabilize the turbulence rather than amplify it. Thus, in summary, the present three-wire measurements appear to be producing more reliable results than the previous single wire-measurements.

Uncertainty estimates were made on the data by two methods. First the sensitivity of the calculations to small changes in primary measured quantities was determined. These calculations showed significantly less error magnification than was determined for the six-orientation single hot-wire method[4]. Additionally, hot-wire signals were analyzed using the two methods of handling data with negative squared quantities discussed earlier in Section 3.1. The difference between data determined in these two manners provides a measure of the uncertanity in the final estimates. A representative sample of the data is shown in Figure 19. Included are the profiles of mean axial velocity, the axial component of turbulence velocity and the $\overline{u'v'}$ component of the turbulent shear stress, measured at x/D=1.0. The solid circles represent estimates in which negative squared quantity data are eliminated from the data set. The open circles are estimates in which individual velocity components (in wire coordinates) are set equal to zero when encountering a negative squared quantity. These two estimates define an anticipated bound for the actual data.

Included on the figures (with the x symbol) are the estimates obtained from the six-orientation single hot-wire measurements[4]. Note that there is very good agreement between the two methods in the estimates of axial mean velocity and axial turbulence velocity. For this comparison, $\overline{u'v'}$ values measured by the six-orientation technique have been assigned the appropriate sign corresponding to the results of the triple-wire study. In the turbulent shear stress estimates, there is typically more scatter in the single wire measurements with indicated magnitudes usually larger than the triple-wire measurements.

A final point to be made regarding the comparison between the two hot-wire methods concerns the ability of the triple-wire technique to produce time series data as opposed to the single-wire technique whose reduced data is always in time averaged form. A detailed discussion on time-series data is presented in the following section.

4.7 Real-time Measurements:

The triple-wire study presented here is unique in the sense that it provides time-series for the velocity vector sensed by the three wire probe. The previously used multi-orientation single hot-wire technique uses the averaged and root-mean-squared fluctuation values of hot-wire voltage for data reduction. The triple-wire data acquisition is automated and signals are digitized using real-time analog to digital converters. The triple-wire technique thus has a definite advantage over the six-orientation single wire method.

Figure 20 shows the time-series of the velocity experienced by one of the three wires. This record was obtained in the swirling confined jet at x/D=1.0, r/D=0.3 with ϕ=38 degrees, and α=90 degrees. The figure shows large variations in velocity occuring at frequencies up to about 200 Hz. Most of the turbulence energy is carried at these low frequencies. In addition, there are large peaks occuring at even lower frequencies such as 20 Hz.

Figure 21 shows the power spectral density of the signal from a single hot-wire in the confined jet flowfield. In this record 1024 points were digitized at a rate of 32 kHz. The plot shows that most of the energy of turbulence is contained in frequencies lower than 1 kHz. A decision was then made to set the data digitization rate at 2.0 kHz for production run experiments.

A review of Figure 20 and 21 suggests that the hot-wire is sensing a considerable amount of low frequency, undoubtly large scale fluid motions. It is possible that these large scale motions are coupling with the acoustic modes of the test chamber. For example, the fundamental plane wave mode for the test chamber is approximately 45 Hz and the spinning modes are correspondingly higher in frequency. These acoustic modes surely cause the recirculation regions to "breathe" producing considerable energy in low frequency fluctuations. This low frequency energy is mostly

deterministic in nature and therefore is not best represented by conventional turbulence models. The triple-wire hot-wire technique developed in this study could be used to conduct a detailed study of the large scale motions and their acoustic interactions in the swirling confined jet flowfield. Such a study would provide valuable information to aid in the interpretation of combustion instabilities in axisymmetric combustors.

5. CONCLUSIONS

5.1 Summary

The measurements of time-mean velocities and shear stresses in a complex three-dimensional flowfield have been carried out using a triple-wire probe. The salient features of the outcome of the present study can be summarized as follows:

1. Mean velocities measured by the triple-wire probe are in very good agreement with measurements performed with a five-hole pitot probe in an identical flowfield.

2. In the non-swirling confined jet, turbulence measurements are in very good agreement with previous measurements performed by Chaturvedi[9] using a conventional x-wire probe.

3. In the swirling confined jet flowfield the turbulence intensities and turbulent shear stress estimates obtained from the triple-wire technique are in general agreement with the corresponding measurements performed with the previous six-orientation single hot-wire method. In fact, the present measurements appear to be more accurate (and hence more reliable) insofar as they retain the time series information lost in the single-wire method.

5.2 Further Study:

In the present study the triple-wire measurements have been performed for a confined jet flowfield with the swirl vane angle ϕ=38 deg. with an expansion angle α=90 deg. The measurements have produced detailed baseline turbulence data which can be used to evaluate the applicability of various turbulence models in this swirling flowfield.

An obvious extension of this work would include a parametric study of the effect of vane angle and expansion angle on the turbulence properties. The ability of the triple-wire probe to perform real-time measurements in complex (swirling) flowfields suggests a detailed examination of velocity transients and their coupling with acoustic modes. This type of study should also be performed with downstream blockage found in realistic combustor geometries.

REFERENCES

1. Lilley, D.G., *"Flowfield Modeling in Practical Combustors: A Review,"* Journal of Energy.Vol. 3, No. 4, 1979.

2. Lilley, D.G. and Rhode, D.L., *"A Computer Code for Swirling Turbulent Axisymmetric Recirculating Flows in Practical Isothermal Combustor Geometries,"* NASA Contractor Report 3442, February 1982.

3. Rhode, D.L., Lilley, D.G. and McLaughlin D.K., *"Mean Flowfields in Axisymmetric Combustor Geometries with Swirl,"* AIAA Paper No. 82-0177, 1982, AIAA Journal (in press).

4. Janjua, S.I., McLaughlin, D.K., Jackson, T.J. and Lilley, D.G., *"Turbulence Measurements in a Confined Jet using a Six-Orientation Hot-Wire Technique,"* AIAA Paper No. 82-1262 AIAA/SAE/ASME 18th Joint Propulsion Conference, June 21-23, 1982, Cleveland, Ohio.

5. Yonuzkurt, S., Crawford, M. and Moffat, R. *"Real-Time Hot-Wire Measurements in Three-Dimensional Flows,"* Symposium on Turbulence, University of Missouri Rolla, October, 1977, pp 265-279.

6. Gaulier, C. *"Measurement of Air Velocity by Means of a Triple Hot-Wire Probe,"* DISA Information No. 21, April 1977, pp 16-20.

7. Jorgensen, F.E., *"Directional Sensitivity of Wire and Fiber Film Probes, An Experimental Study,"* DISA Information No. 11, May 1971, pp. 31-37.

8. Yoon, H.K., *"Five-Hole Pitot Probe Time-Mean Velocity Measurements in Confined Swirling Flows,"* M.S. Thesis, Oklahoma State University, June 1982.

9. Chaturvedi, M.D., *"Flow Characteristics of Axisymmetric Expansions,"* Proceedings, Journal of Hydraulic Division ASCE, 99, No HY3, pp. 61-92, 1963.

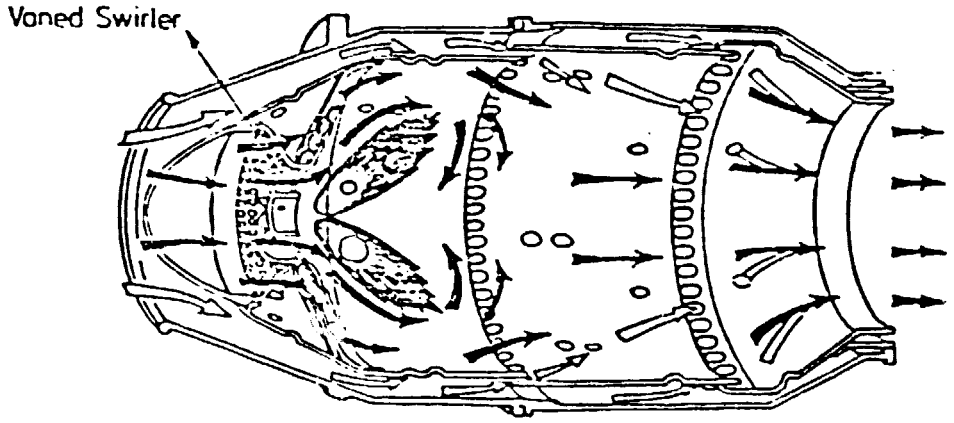

Figure 1. Typical Axisymmetric Combustion Chamber of a Gas Turbine Engine.

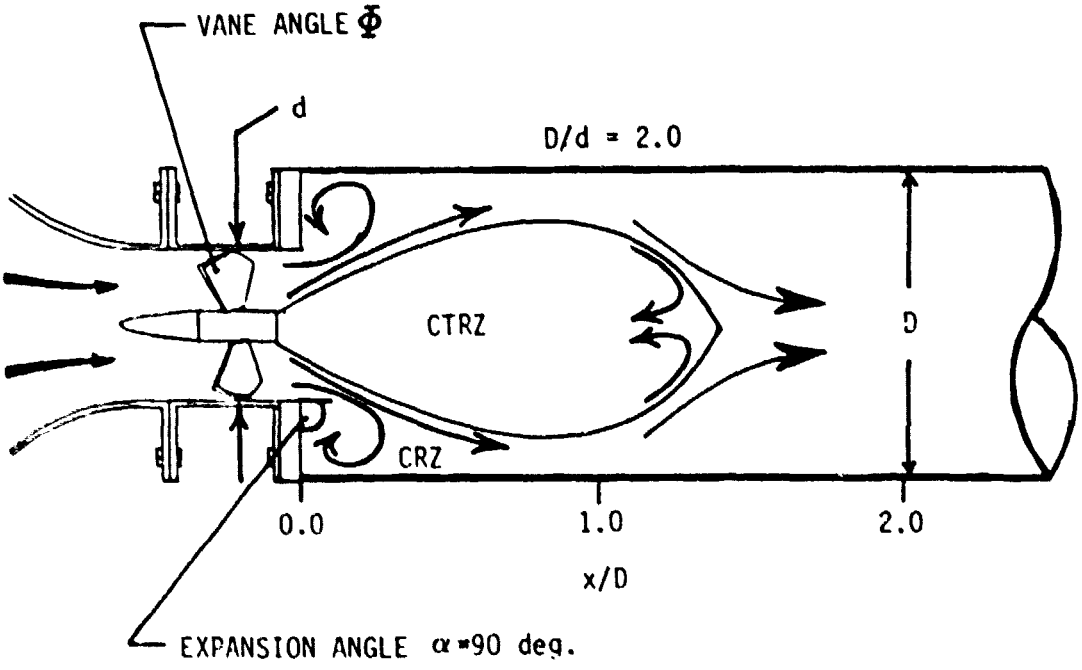

CRZ - Corner Recirculation Zone

CTRZ - Central Toroidal Recirculation Zone

Figure 2. Idealized Combustor Flowfield.

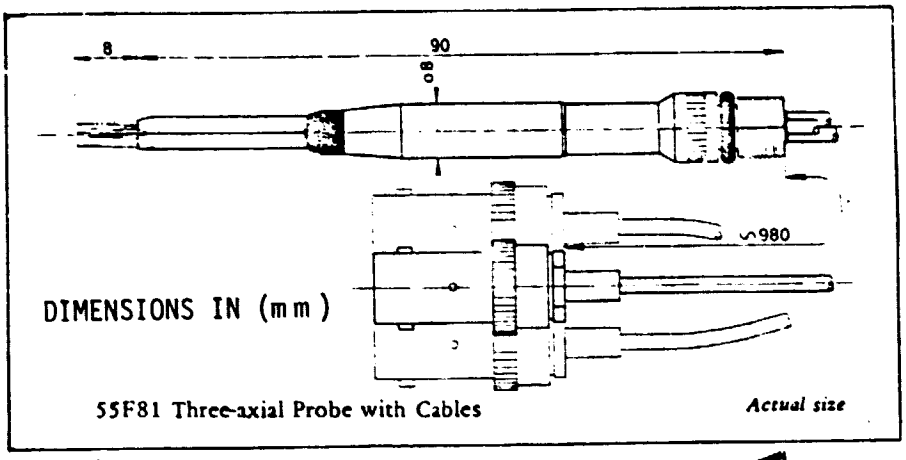

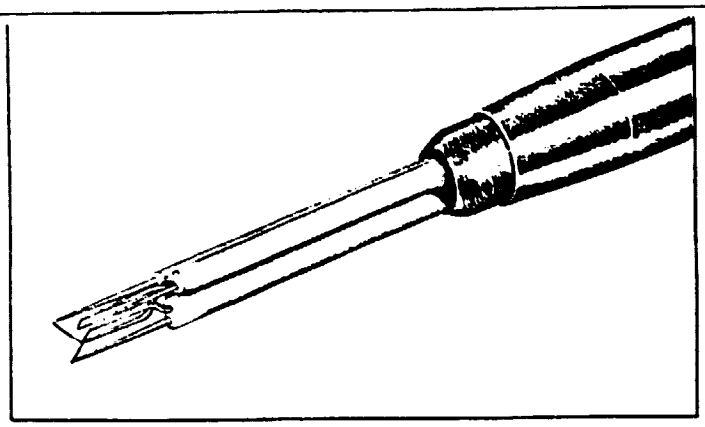

Figure 3. The Triple-Wire Probe.

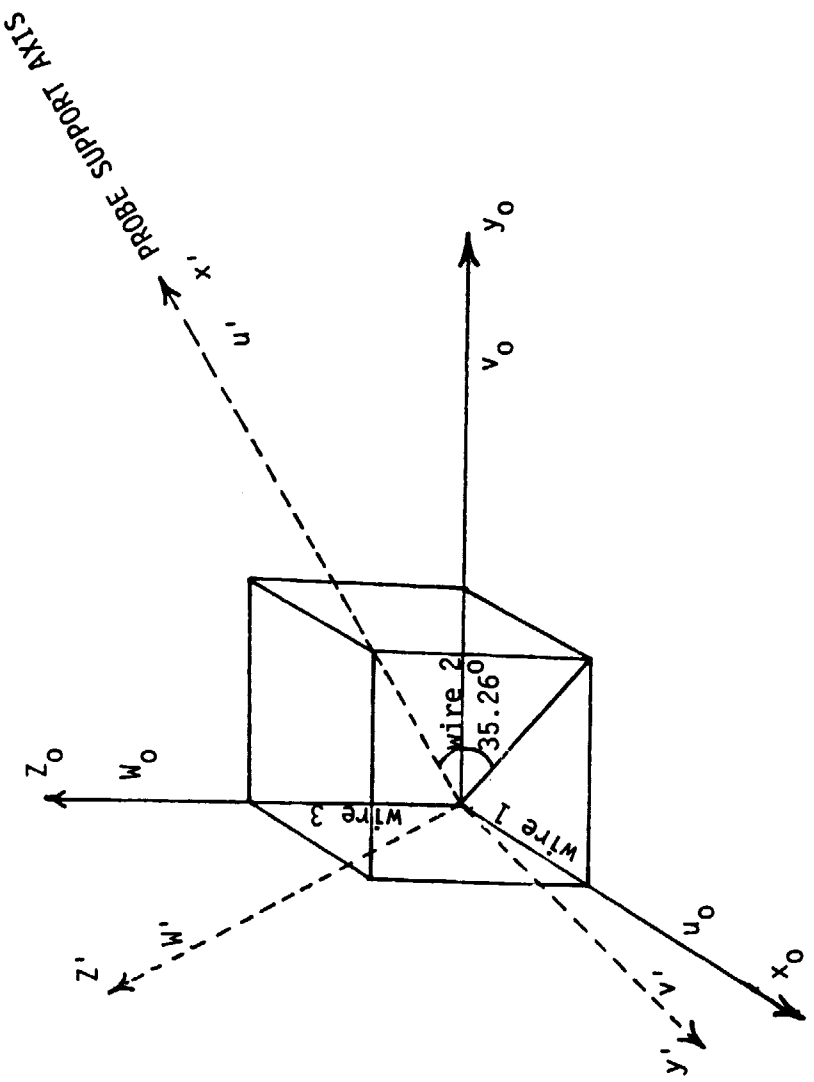

Figure 4. Wire Array with Respect to the Support Axis.

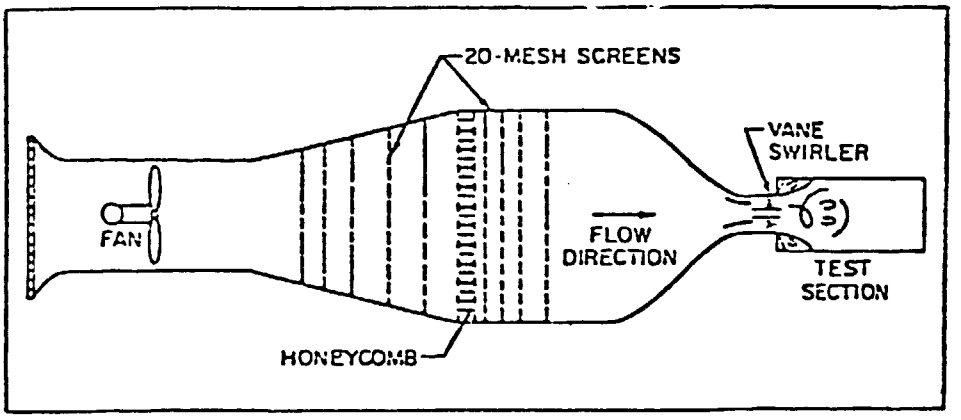

Figure 5. Schematic of Overall Facility.

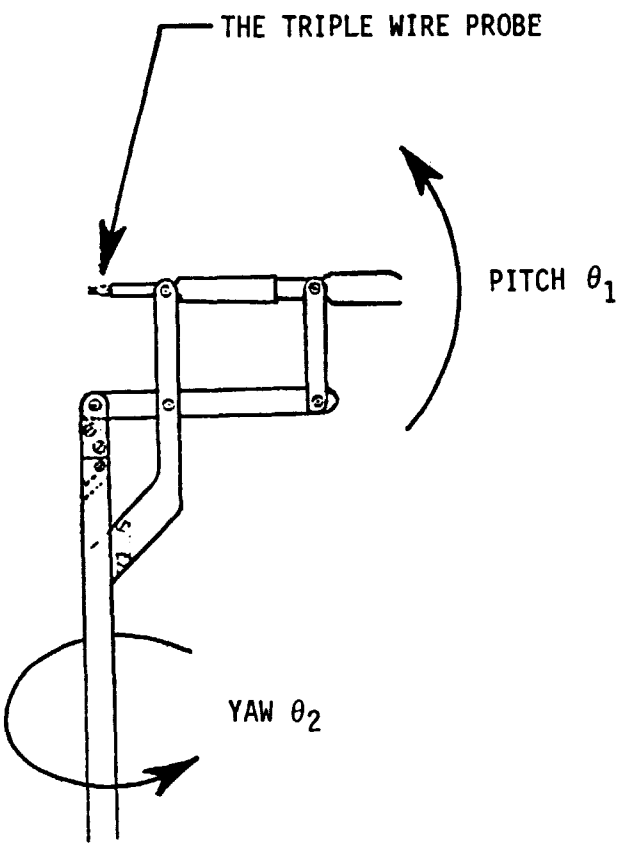

Figure 6. The Three Dimensional Probe Drive.

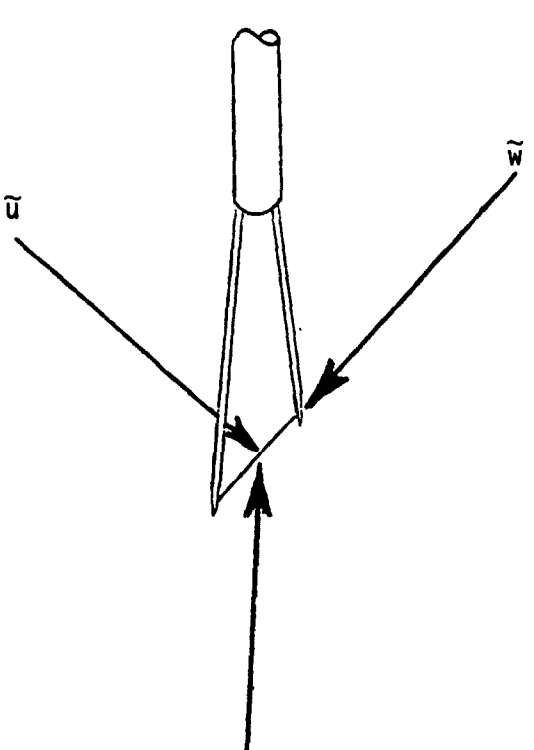

Figure 7. Coordinate System Defined by a Single Wire.

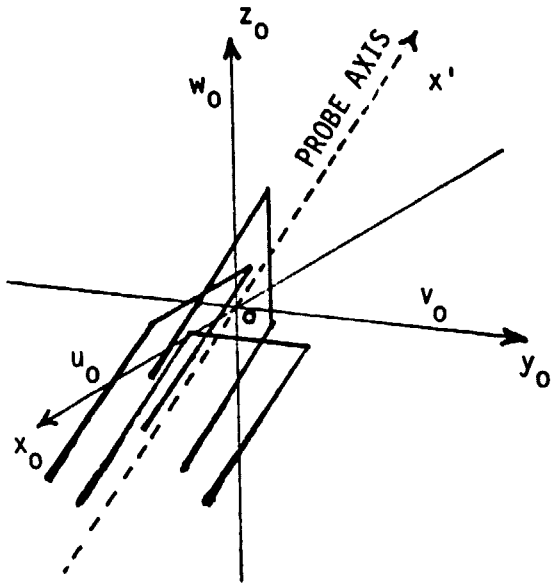

Figure 8. Coordinate System Defined by the Three Wires.

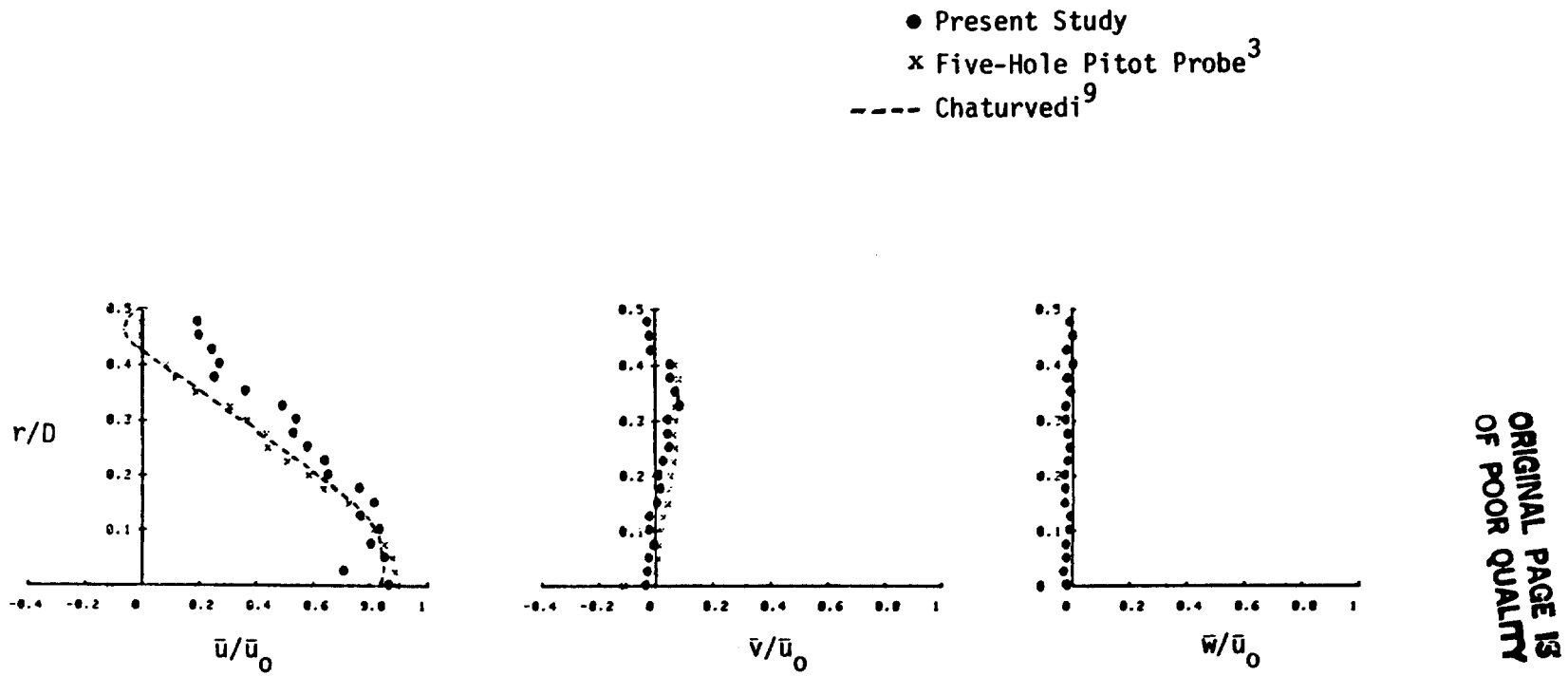

Figure 9. Non-Swirling Flowfield at x/D=2.0 with $\phi=0^o$ and $\alpha=90^o$.

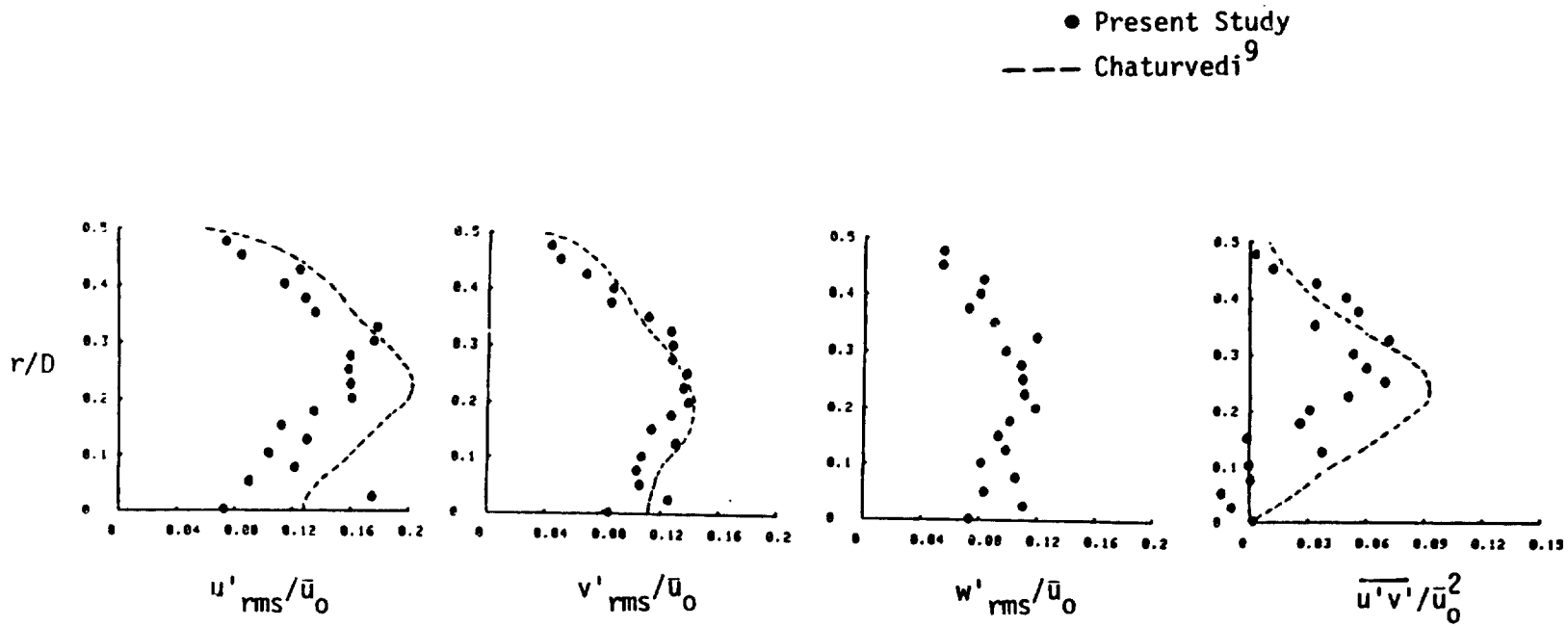

Figure 9. (Cont'd)

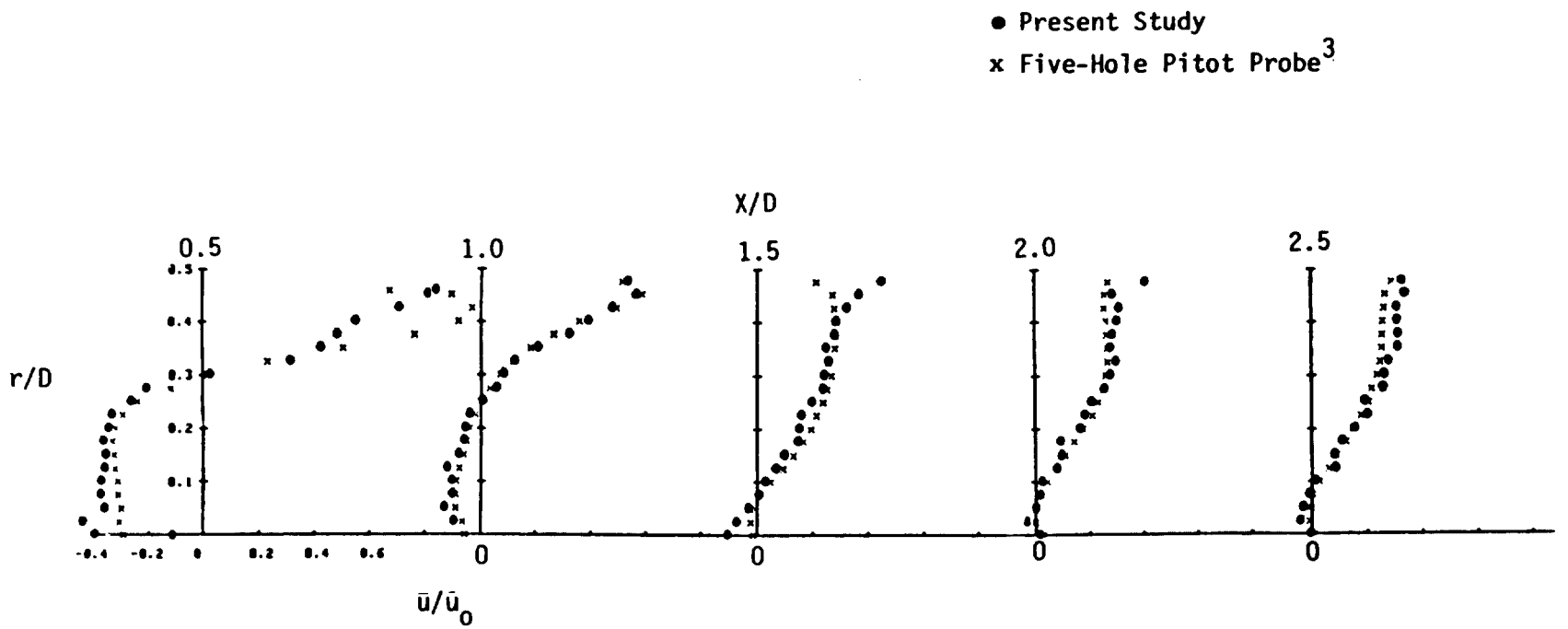

Figure 10. Radial Distribution of Mean Axial Velocity in Swirling Confined Jet with $\Phi=38^{o}$ and $\alpha=90^{o}$.

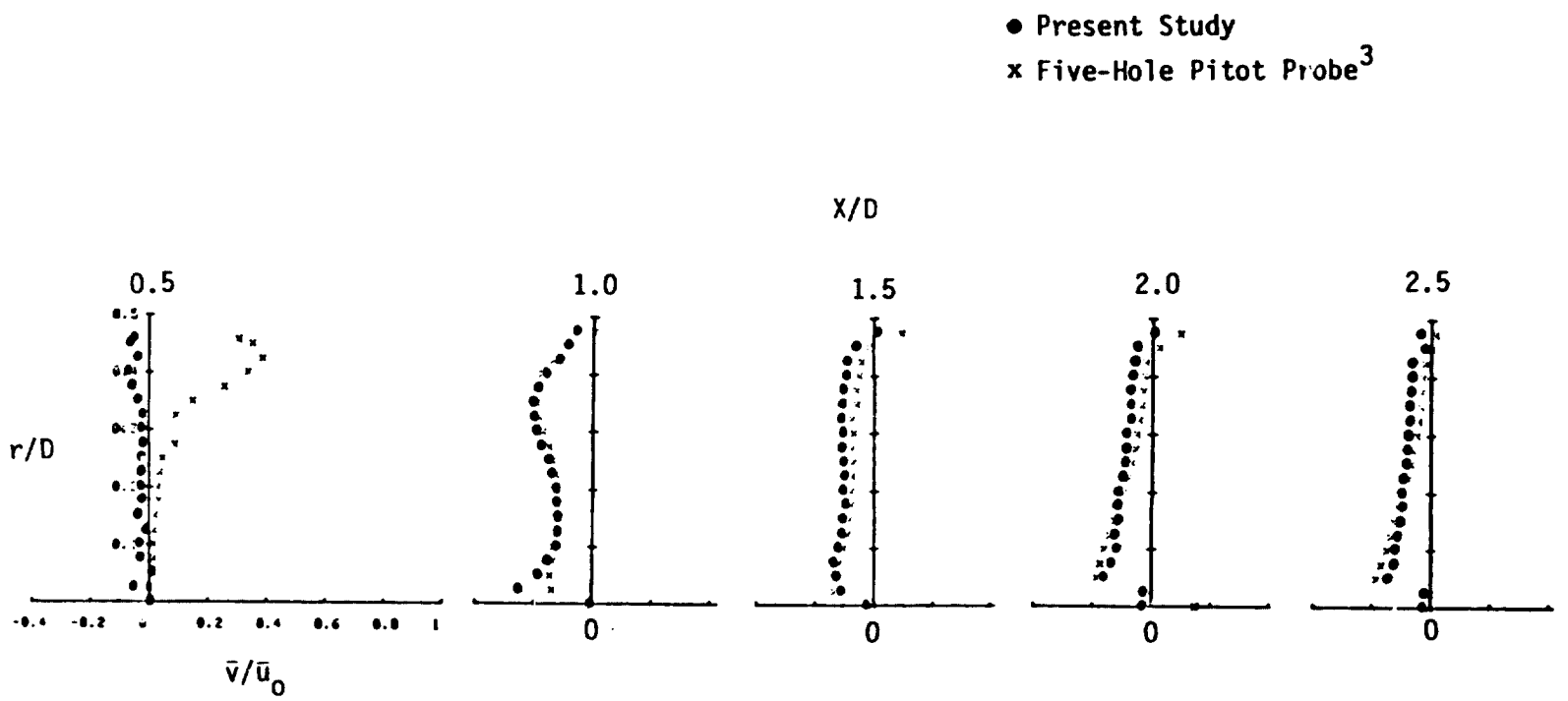

Figure 11. Radial Distribution of Mean Radial Velocity in Swirling Confined Jet with Φ=38° and α=90°.

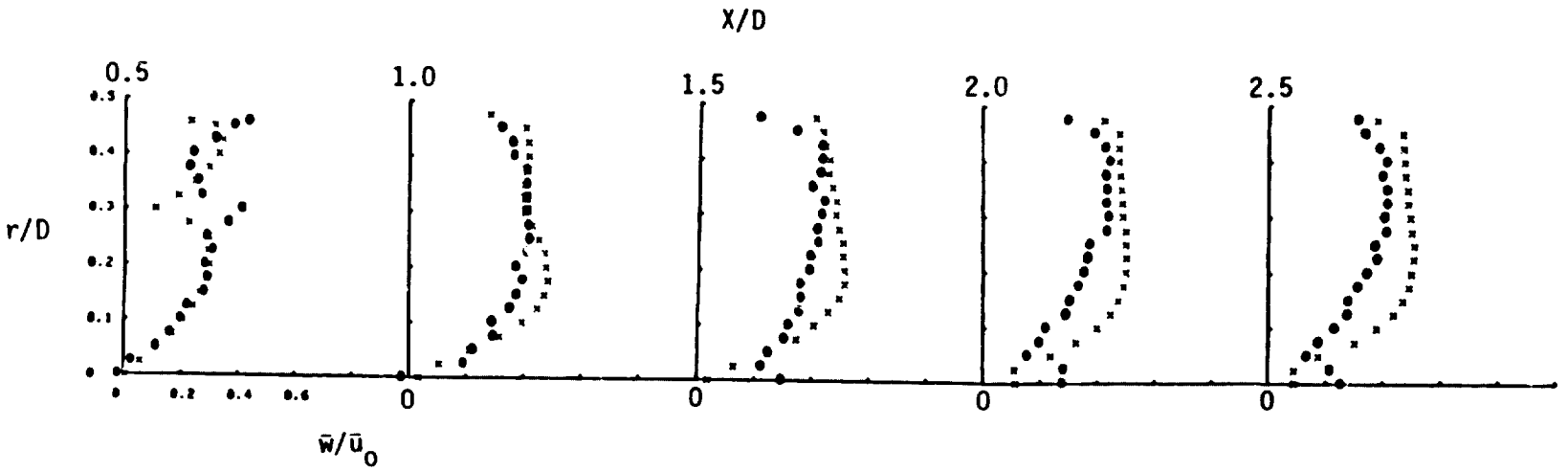

Figure 12. Radial Distribution of Mean Azimuthal Velocity in Swirling Confined Jet with $\Phi=38^o$ and $\alpha=90^o$.

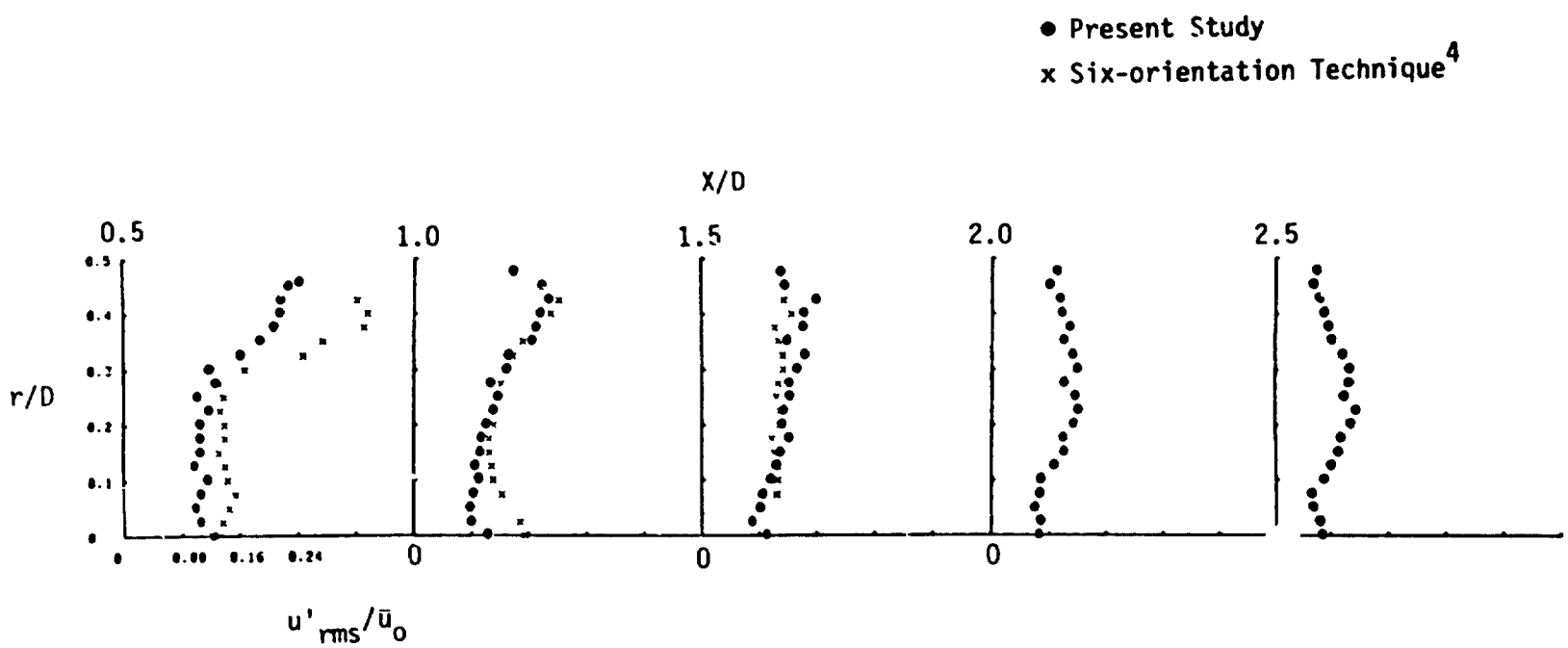

Figure 13. Radial Distribution of Axial Turbulence Intensity in Swirling Confined Jet with $\Phi=38^0$ and $\alpha=90^0$.

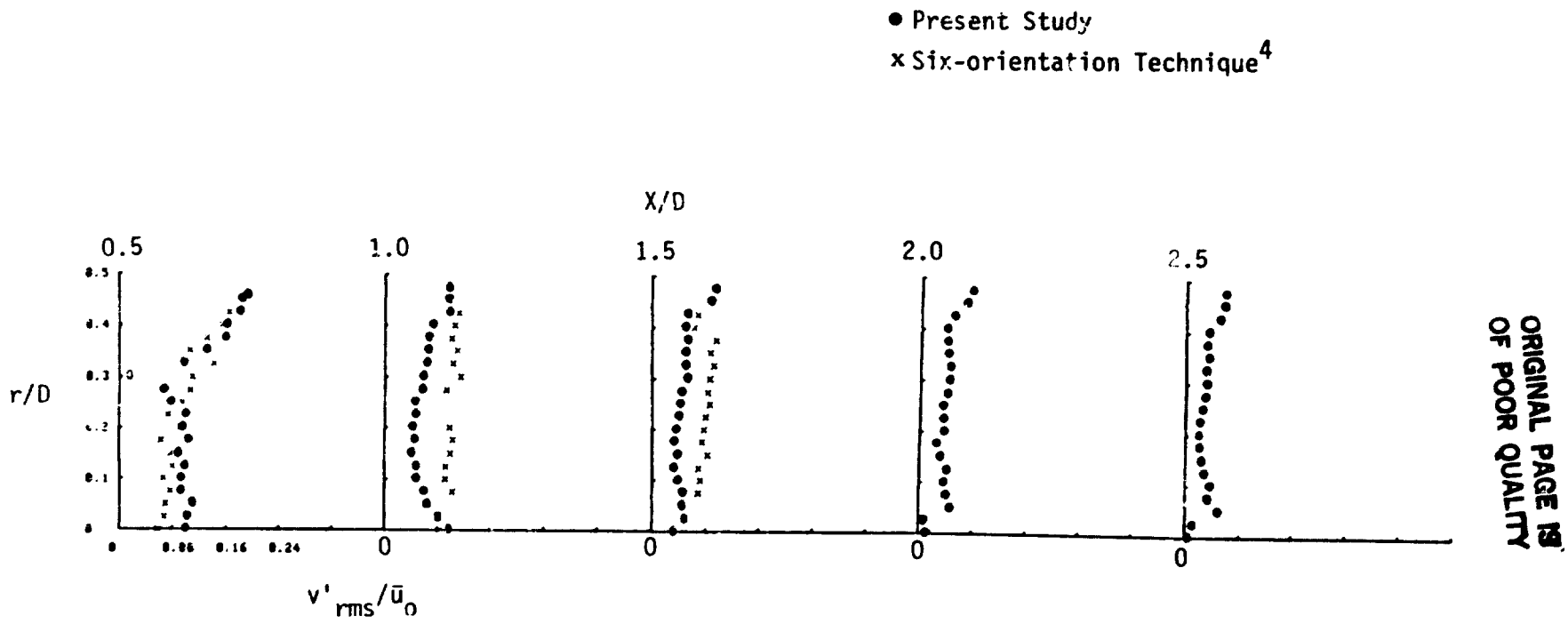

Figure 14. Radial Distribution of Radial Turbulence Intensity in Swirling Confined Jet with $\Phi=38^{o}$ and $x=90^{o}$.

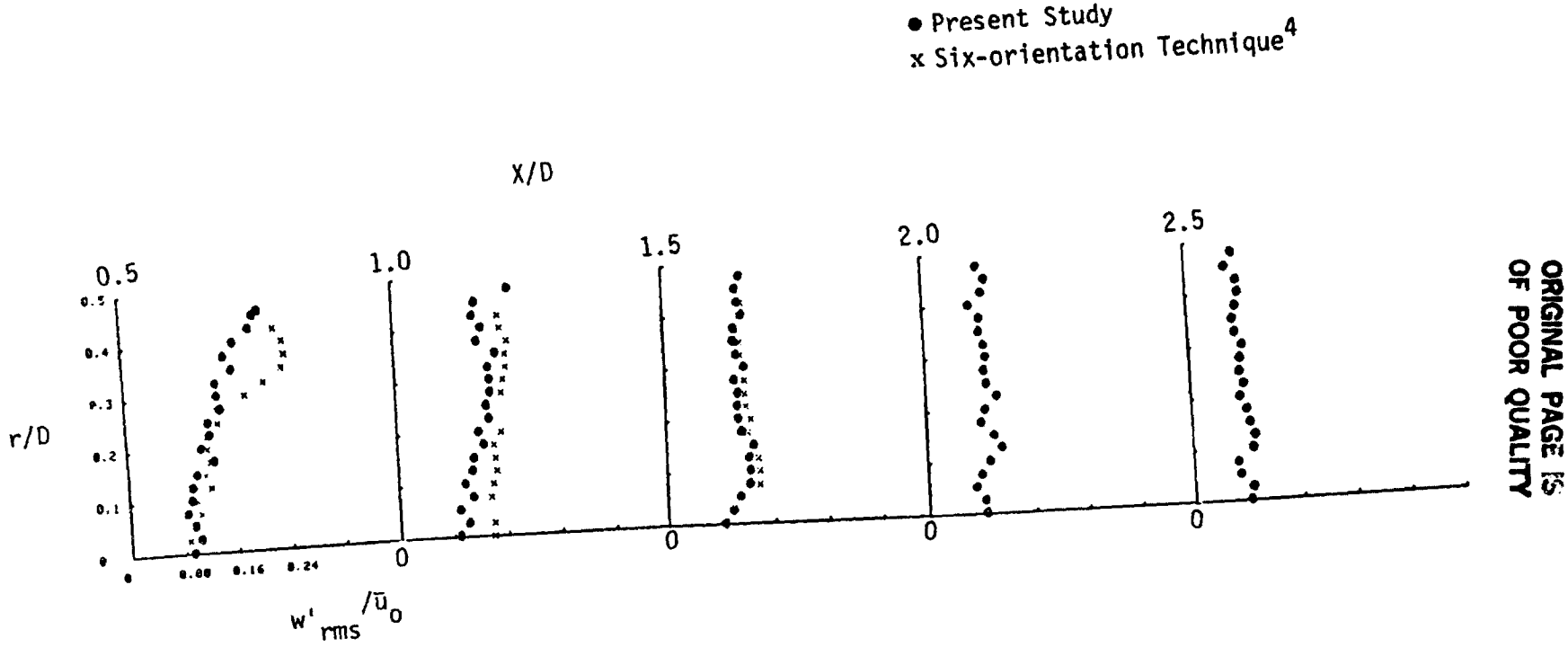

Figure 15. Radial Distribution of Azimuthal Turbulence Intensity in Swirling Confined Jet with $\Phi=38^{o}$ and $\alpha=90^{o}$.

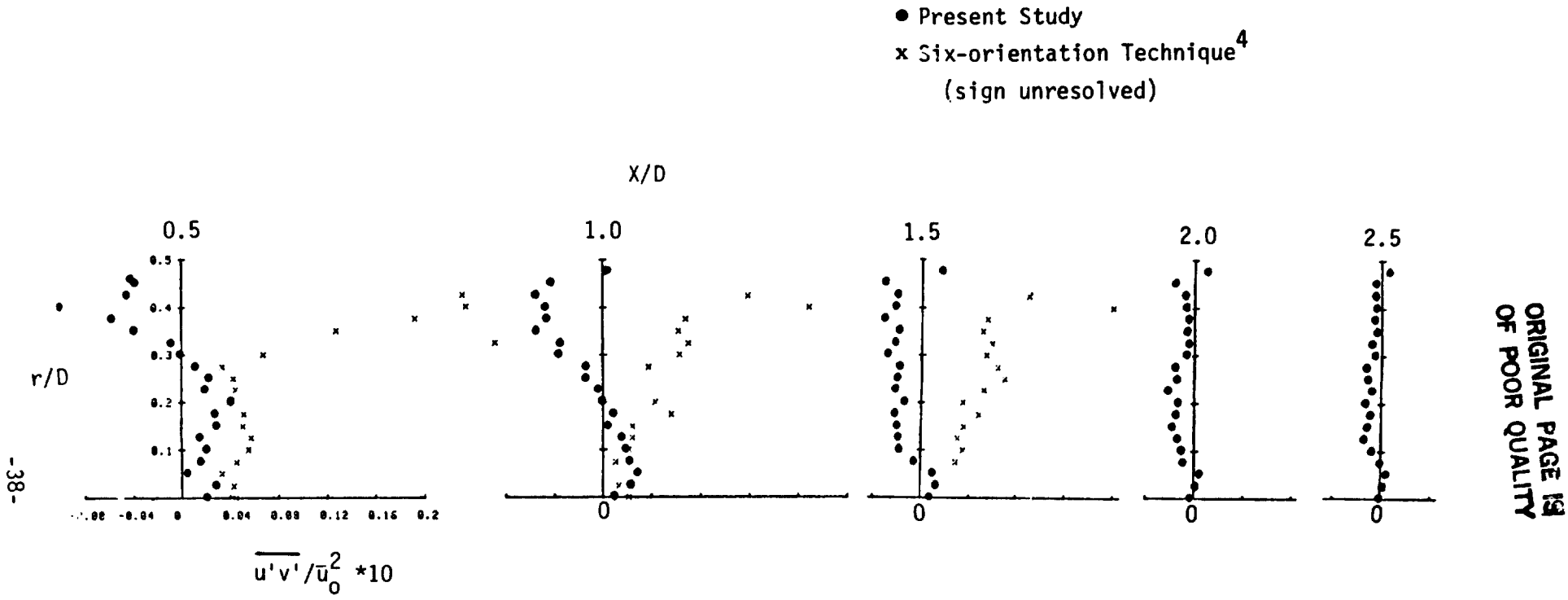

Figure 16. Radial Distribution of Shear Stress $\overline{u'v'}$ in Swirling Confined Jet with $\Phi=38^o$ and $\alpha=90^o$.

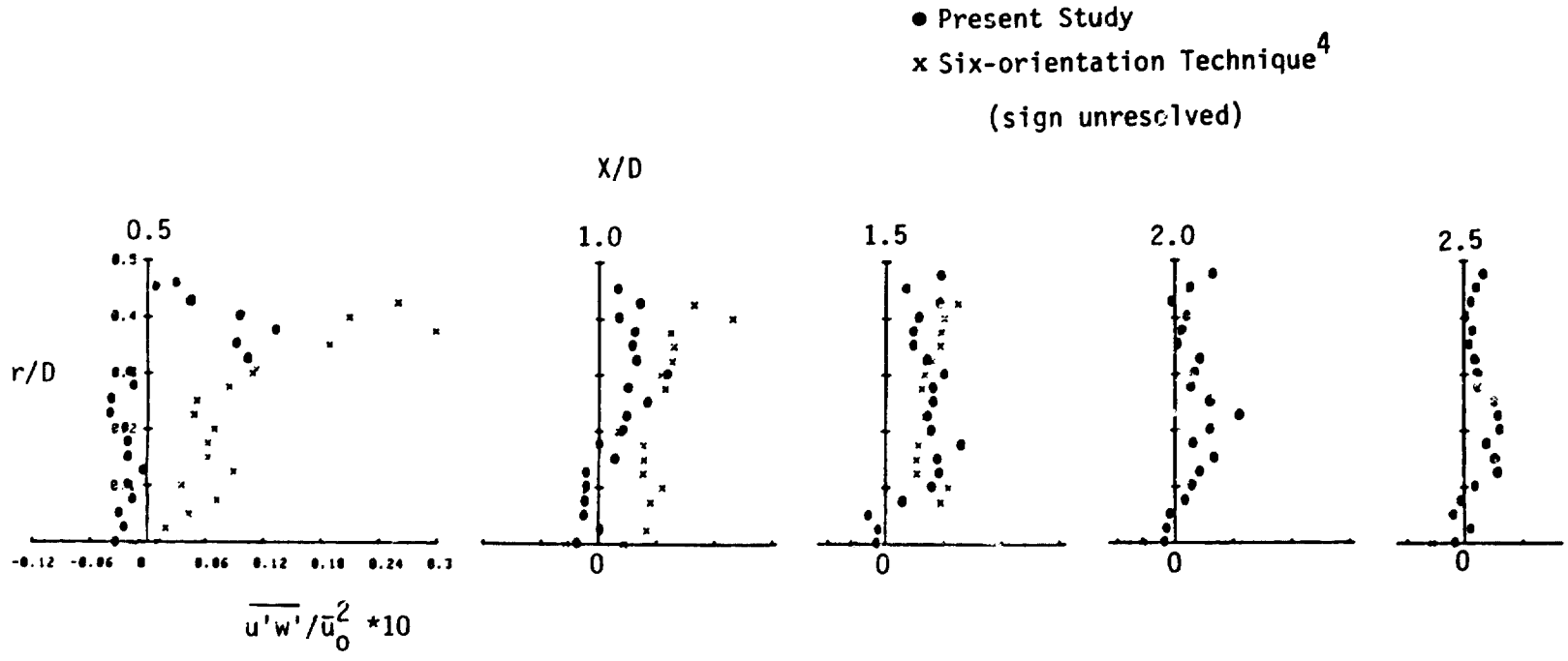

Figure 17. Radial Distribution of Shear Stress $\overline{u'w'}$ in Swirling Confined Jet with $\Phi=38^o$ and $\alpha=90^o$.

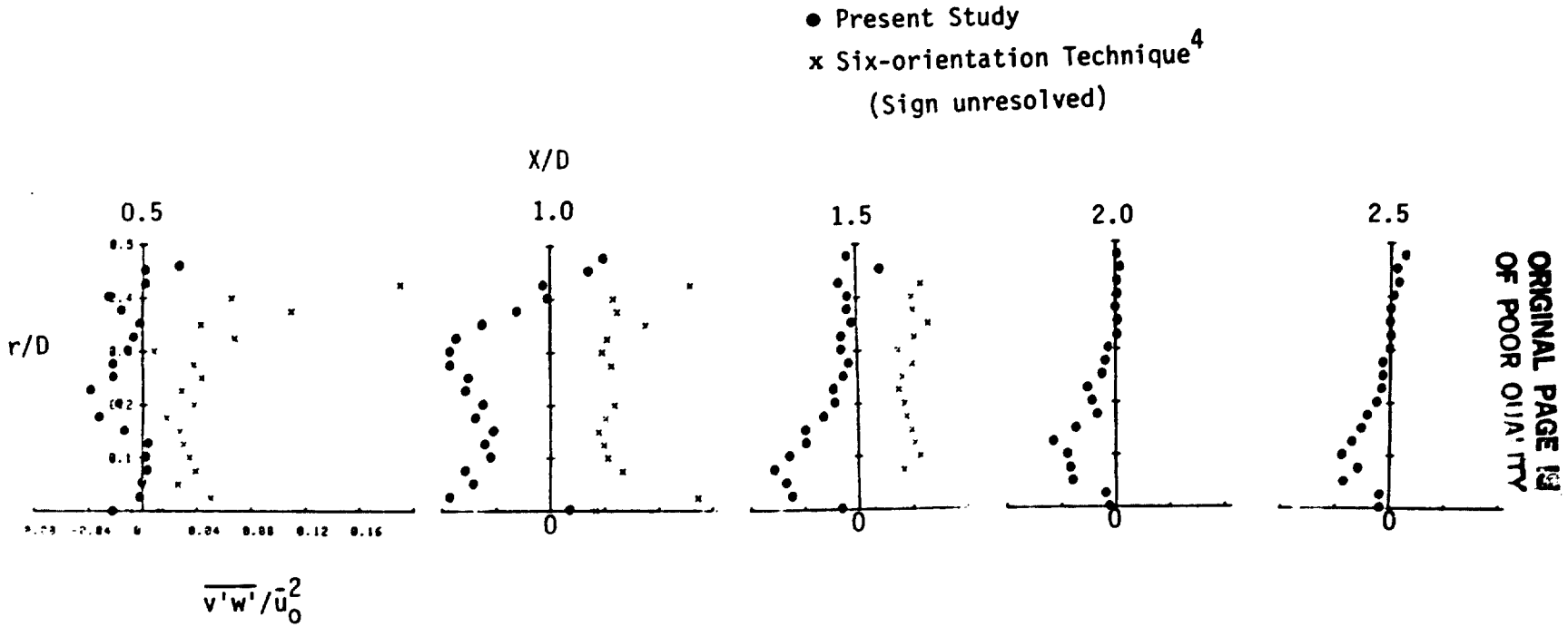

Figure 18. Radial Distribution of Shear Stress $\overline{v'w'}$ in Swirling Confined Jet with $\Phi=38^o$ and $\alpha=90^o$.

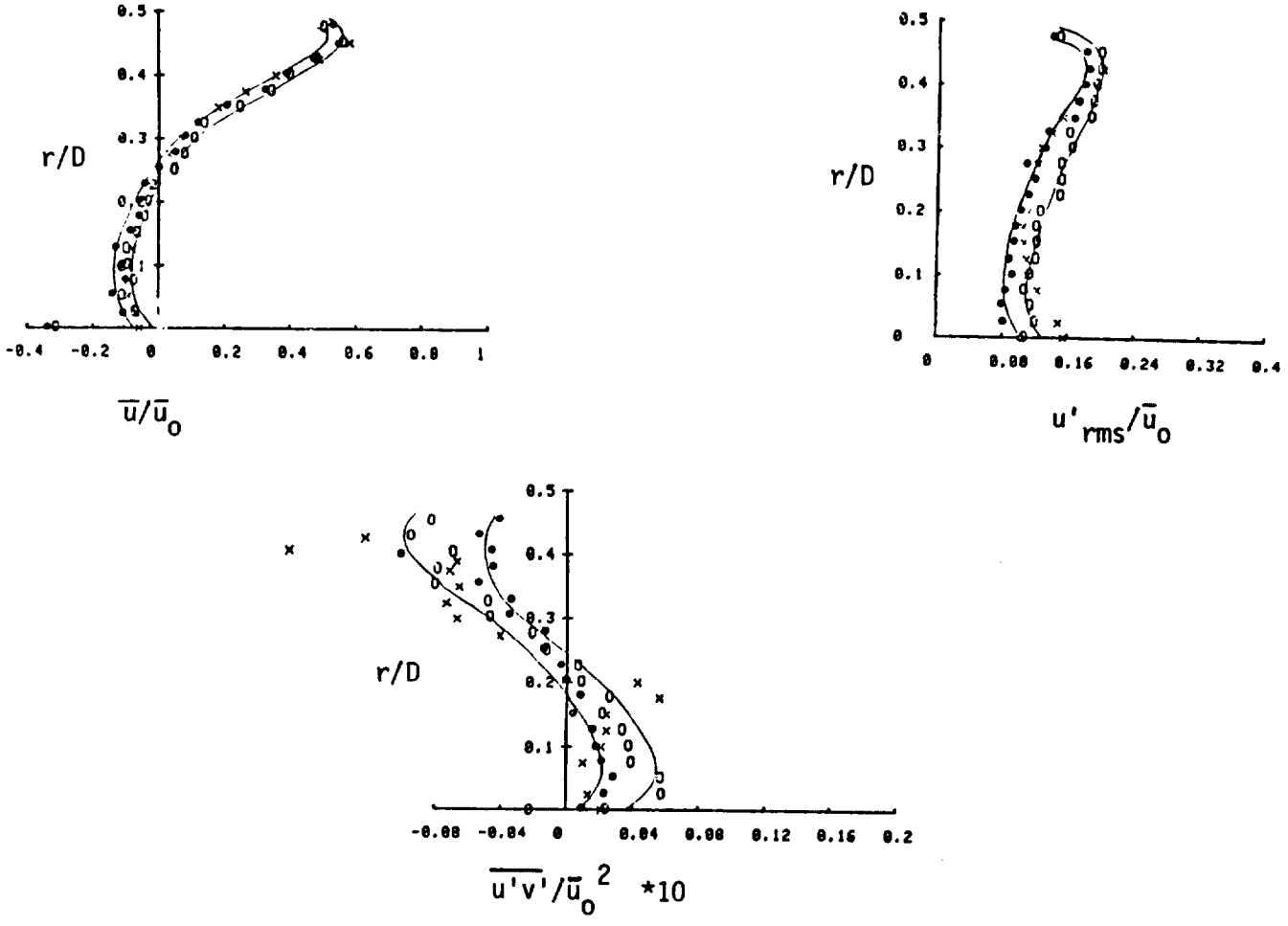

Figure 19. Bands of Uncertainities in Measurements of Mean and Turbulence Quantities Measured at x/D = 1.0 with $\Phi = 38^o$ and $\alpha = 90^o$.

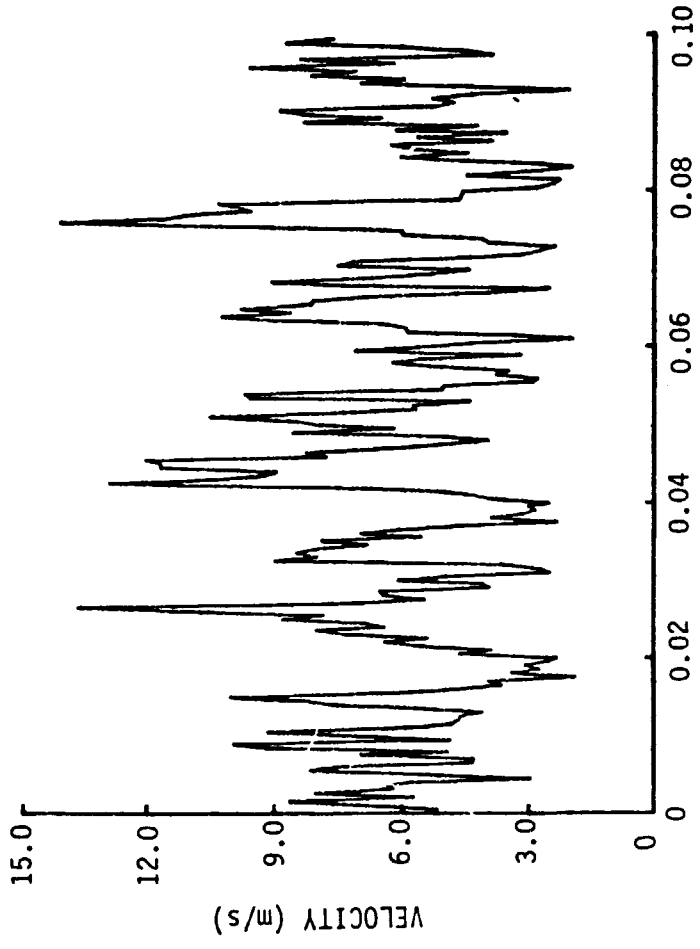

Figure 20. Time-Series of Velocity Experienced by one of the Wires in Swirling Flow at x/D = 1.0 and r/D = 0.3 with $\phi = 38^{0}$ and $\alpha = 90^{0}$.

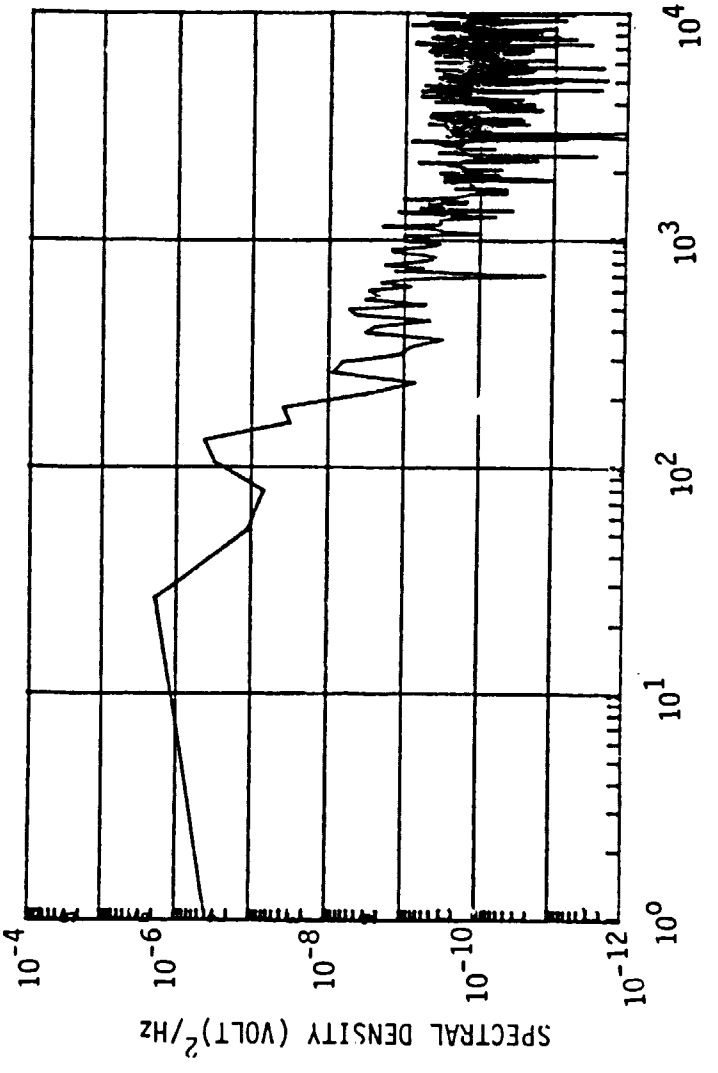

Figure 21. Power Spectral Density Plot for Non-Swirling Confined Jet Flow, at x/D = 1.0 and r/D = 0, with $\Phi = 0^{0}$.

APPENDIX A

Turbulence Measurement In A Confined Jet Using A Six-Orientation Hot-Wire Probe Technique

AIAA-82-1262

Turbulence Measurements In A Confined Jet Using A Six-Orientation Hot-Wire Probe Technique

S. I. Janjua and D. K. McLaughlin, Dynamics Technology, Inc., Torrance, CA,

T. W. Jackson and D. G. Lilley, Oklahoma State Univ., Stillwater, OK

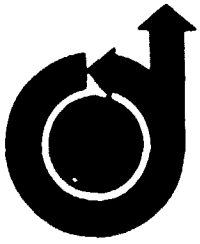

AIAA/SAE/ASME
18th Joint Propulsion Conference
June 21-23, 1982/Cleveland, Ohio

TURBULENCE MEASUREMENTS IN A CONFINED JET USING A SIX-ORIENTATION HOT-WIRE PROBE TECHNIQUE

S. I. Janjua* and D. K. McLaughlin**
Dynamics Technology, Inc., Torrance, California

and

T. Jackson† and D. G. Lilley††
Oklahoma State University, Stillwater, OK.

Abstract

The six-orientation single hot-wire technique has been applied to the complex flowfield of a swirling, confined jet. This flowfield, which contains a rapid expansion with resulting recirculation regions, is typical of those found in gas turbine engines and ramjet combustors. The present study focusses on turbulence measurements in such a flowfield in the absence of chemical reaction.

A modification to the six-orientation hot-wire technique developed by King has been made, which incorporates the determination of turbulent shear stresses (in addition to normal stresses) and ensemble averaging of redundant turbulence output quantities. With this technique, flowfield surveys have been performed in both swirling and nonswirling axisymmetric confined jets. Where independent data exist, comparisons have been made which demonstrate the reliability of the technique. Finally, a sensitivity analysis of the data reduction technique has been completed which forms the major ingredient in an uncertainty analysis.

Nomenclature

A,B,C	Calibration constants in Equation 1
AO,BO,CO	Cooling velocity functions in Table 1
D	Test section diameter
d	Inlet nozzle diameter
E	Hot-wire voltage
U	Velocity function for axial velocity
W	Velocity function for azimuthal velocity
V	Velocity function for radial velocity
G	Pitch factor
K	Yaw factor
$K_{z_p z_Q}$	Covariance for cooling velocities Z_p, and Z_Q
P,Q,R	Selected hot-wire probe positions
Re_d	Inlet Reynolds number
u	Axial velocity } in
v	Radial velocity } coordinates
w	Azimuthal (swirl) velocity } on facility
$\tilde{u},\tilde{w},\tilde{v}$	Three components of velocity in probe coordinates defined by Figure 5
x,r,θ	Axial, radial, azimuthal cylindrical polar coordinates
Z	Effective cooling velocity acting on a wire
α	Side-wall expansion angle
$\gamma_{Z_i Z_j}$	Correlation coefficient (estimated) between cooling velocities of adjacent wire orientations
σ^2	Variance of a given quantity
ϕ	Inverse function of calibration equation
Φ	Swirl vane angle

Subscripts

1,2,3,4,5,6	Refers to the six probe measuring positions
i,j	Dummy indicies which take the values 1 to 3
P,Q,R	Refers to the three selected measuring positions
rms	Root-mean-squared quantity

Superscripts

¯	Time-mean average
'	Fluctuating quantity

1. Introduction

1.1 The Gas Turbine Combustor Flowfield

Recent emphasis on fuel economy and pollutant suppression has sparked a renewed interest in gas turbine combustor analysis. A typical axisymmetric gas turbine engine combustor is shown in Figure 1. Flowfields within such combustors typically have a rapid expansion and strong swirl imparted to the incoming air, which result in corner and central recirculation regions. The swirling, recirculating, turbulent flows within combustors present one of the more difficult fluid dynamic problems to analyze. This complexity is increased many fold by the processes of combustion and heat transfer within the flowfield. Despite the complexity of combustor flows, significant progress is being made in their analysis.[1]

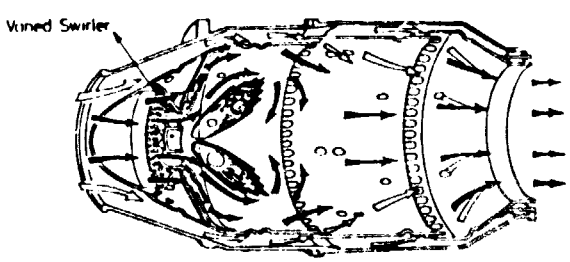

Figure 1. Axisymmetric Combustor of a Gas Turbine Engine

* Research Engineer, Member AIAA
** Senior Research Scientist, Member AIAA
† Graduate Student, Student Member AIAA
†† Professor, Associate Fellow AIAA

The present paper reports on research which is part of an extensive experimental and computational study of gas turbine flowfields in the absence of combustion. Figure 2 shows the characteristics of the simplified flowfield being investigated. Flow enters through a jet of diameter d into a tube of diameter D, after being expanded through an angle α. Before entering the tube, the flow may be swirled by a swirler located upstream of the inlet plane. Shown schematically are the corner recirculation zone (CRZ) and the central toroidal recirculation zone (CTRZ) which are typically present in these flows.

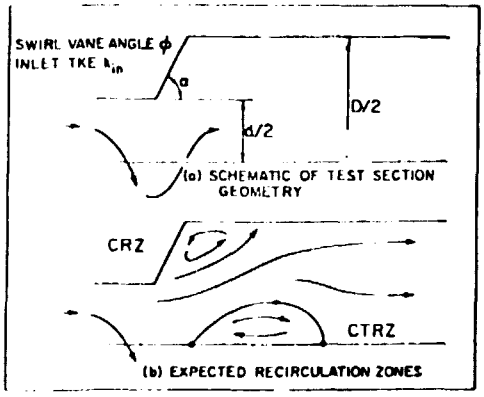

Figure 2. Idealized Combustor Flowfield

The swirling confined jet flowfield shown in Figure 1 is being investigated at Oklahoma State University and at Dynamics Technology, with various methods of approach. Analytically, a computer program (STARPIC) has been assembled which is designed specifically to calculate the swirling confined jet flowfields.[2] Experimentally, a series of flow visualization experiments coupled with 5-hole pitot probe measurements have been used to characterize the time-mean flowfield.[3] Hot-wire measurements of the turbulence properties are also being conducted. This paper reports on the initial results of the hot-wire measurements in the confined jet flowfield.

Several studies on time-mean flowfields of the type just described have been carried out using various turbulence measuring techniques.[4-10] Unfortunately, most of the techniques used do not give complete and detailed information about the flow in terms of all its time-mean and turbulence quantities. In addition, no experiments have been performed on the specific geometry of the present study in the presence of inlet swirl. To develop further the flowfield computational techniques, including the turbulence modeling, there is a strong need to obtain experimental estimates of the turbulence and mean flow quantities in such flows.

1.2 The Turbulence Measurement Problem

Turbulence measurement in a complex flowfield has always been a complicated problem encountered by engineers. In the past, turbulence phenomena have been discussed by various authors in detail and various methods of turbulence measurements have been suggested.[11-13] One of the most widely used instruments to obtain turbulence quantities is the hot-wire anemometer, the most common of which is a single hot-wire. When used at a single orientation and in a two-dimensional flow with a predominant flow direction, a single hot-wire can measure the streamwise components of the time-mean velocity and the root-mean-square velocity fluctuation at a particular location in the flowfield. A two-wire probe can be used to determine the time-mean velocities, streamwise and cross stream turbulence intensities, and the cross correlation between the two components of the velocity fluctuations.[14-15]

Hot-wire measurements in complex three-dimensional flowfields are considerably more difficult than in one- or two-dimensional flowfields in which the mean flow is predominantly in one direction. To measure the three velocities and their corresponding fluctuating components in a three-dimensional flowfield such as encountered in combustor simulators, there are two methods that can be employed at a point in the flowfield:

1) A three-wire probe used with a single orientation.

2) A single- or double-wire probe used with multi-orientation.

The three-wire probe technique permits the necessary simultaneous measurements from which three instantaneous velocity components can be determined. The appropriate signal processing can produce estimates of mean velocity components and normal and shear turbulent stresses (such as $\overline{u'^2}$ and $\overline{u'v'}$).

The three-hot-wire probe technique is significantly more complex than the single wire multi-orientation techniques. A multi-dimensional probe drive is required to orient the probe in approximately the mean flow direction. Also, sophisticated signal processing electronics is required to handle the three instantaneous hot-wire voltages. Finally, the three-wire probe typically has less spatial resolution in comparison with a single wire probe.

Multi-orientation of a single hot-wire is a novel way to measure the three components of a velocity vector and their fluctuating components. A method devised by Dvorak and Syred[16] uses a single normal hot-wire oriented at three different positions such that the center one is separated by 45 degrees from the other two. The velocity vector at a location is related to the three orthogonal components using pitch and yaw factors as defined by Jorgensen.[17] The data are obtained in the form of mean and root-mean-square voltages at each orientation. However, the measurements done with a single wire do not supply all the information needed to obtain the turbulence quantities. Therefore, in addition to a single wire, Dvorak and Syred used a cross-wire probe to obtain the covariances between the voltages obtained at adjacent hot-wire orientations.

King[18] modified the technique developed by Dvorak and Syred. His method calls for a normal hot-wire to be oriented through six different positions, each orientation separated by 30 degrees from the adjacent one. Mean and root-mean-square

voltages are measured at each orientation. The data reduction is performed using some assumptions regarding the statistical nature of turbulence, making it possible to solve for the three time-mean velocities, the three normal turbulent stresses, and the three turbulent shear stresses.

1.3 The Scope of the Present Study

In the present study, the six-orientation single normal hot-wire technique is being employed to obtain the turbulence quantities in the combustor simulator confined jet flowfield. Measurements have been carried out for both swirling and nonswirling flow with expansion angles of 90 degrees (sudden expansion) and 45 degrees (gradual expansion). Only the 90 degree angle data are presented here and the Reynolds number of the inlet flow is = 5 x 10^4 which is comparable with aircraft combustor flows (although our experiments are performed in nonreacting flows). The data reduction procedure extends King's technique to obtain turbulent shear and normal stresses using six basic response equations representing the six orientations of a normal hot-wire positioned in the flowfield. Certain modifications are made in the procedure to calculate covariances which are an integral part of the data reduction procedure. An uncertainty analysis is performed on the technique which reveals the sensitivity of this technique to various input parameters discussed in the later parts of this paper. Some of the turbulence quantities obtained are compared with measurements performed by Chaturvedi[5] using a crossed-wire probe in a corresponding flow situation.

2. Experimental Facility and Instrumentation

2.1 Idealized Flowfield

The facility, designed and built at Oklahoma State University, is a simulation of a typical axisymmetric combustion chamber of a gas turbine engine shown in Figure 1. The schematic of the test facility with the idealized flowfield is shown in Figure 3. Ambient air enters the low-speed wind tunnel through a foam air filter. The air then flows through an axial flow fan driven by a 5 h.p. varidrive motor. Thus, the flow rate can be varied for different test conditions. The flow passes through a turbulence management section which has two fine-mesh screens, a 12.7 cm length of packed straws, and five more fine-mesh screens.

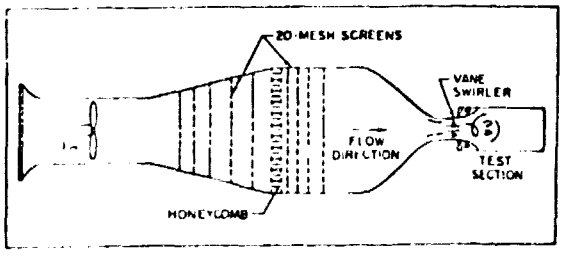

Figure 3. Schematic of the Experimental Facility

The axisymmetric nozzle was designed to produce a minimum adverse pressure gradient on the boundary layer to avoid flow unsteadiness associated with local separation regions. The area ratio of the cross sections of the turbulence management section to that of the nozzle throat is approximately 22.5. The diameter, d, of the nozzle throat is approximately 15 cm.

The test section is composed of a swirler (optional), an expansion block, and a long plexiglass tube. The expansion block, attached after the swirler, is a 30 cm diameter annular disk of wood. At present, there are three expansion blocks, and the appropriate choice gives α = 90, 70, or 45 degrees. The flow is expanded into a plexiglass tube of diameter, D, of 30 cm, thus giving a diameter expansion ratio (D/d) of 2. The test chamber has no film cooling holes or dilution air holes, and the chamber wall of the test section is a constant diameter pipe.

2.2 Hot-Wire Instrumentation

The anemometer used for the present study is DISA* type 55M01, CTA standard bridge. A normal hot-wire probe, DISA type 55P01, is used in the experiments. This probe has two prongs set approximately 3 mm apart which support a 5 μm diameter wire which is gold plated near the prongs to reduce end effects and strengthen the wire. The mean voltage is measured with a Hickok Digital Systems, Model DP100, integrating voltmeter and the root-mean-square voltage fluctuation is measured using a Hewlett Packard, Model 400 HK, AC voltmeter.

The hot-wire is supported in the facility by a traversing mechanism shown schematically in Figure 4. It consists of a base that is modified to mount on the plexiglass tube of the test section at various axial locations. The hot-wire probe is inserted into the tube through a rotary vernier and the base. The rotary vernier is attached to a slide which can traverse across the flow chamber. Thus, it is possible for the probe to be traversed to any radial location at selected downstream locations in the flowfield and to be rotated through 180 degrees.

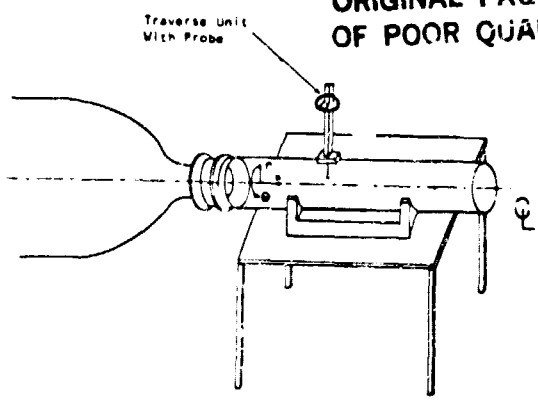

Figure 4. Hot-Wire Probe Mounted on the Test Section

* Provided for information and not necessarily a product endorsement.

2.3 Calibration Nozzle

The hot-wire is calibrated in a small air jet. The facility consists of a compressed air line, which delivers the desired flow rate through a small pressure regulator and a Fisher and Porter Model 10A1735A rotameter. The jet housing consists of an effective flow management section followed by a contoured nozzle with a 3.5 cm diameter throat. A rotary table is used to hold the probe while it is being calibrated in three different orientations.

3. Hot-Wire Data Analysis

3.1 Hot-Wire Response Equations

The six-orientation hot-wire technique requires a single, straight, hot-wire to be calibrated for three different flow directions in order to determine the directional sensitivity of such a probe. The three directions and three typical calibration curves are shown in Figure 5. In these relations, tildes signify components of the instantaneous velocity vector in coordinates on the probe. Each of the three calibration curves is obtained with zero velocity in the other two directions. The calibration curves demonstrate that the hot-wire is most efficiently cooled when the flow is in the direction of the $\tilde{u}$ component, whereas, the wire is most inefficiently cooled when the flow is in the direction of the $\tilde{w}$ component. Each of the calibration curves follows a second order, least square fit of the form:

$$E_i^2 = A_i + B_i \tilde{u}_i^{1/2} + C_i \tilde{u}_i \qquad (1)$$

which is an extension of the commonly used King's law. In this equation, A_i, B_i, and C_i are calibration constants and $\tilde{u}_i$ can take on a value of $\tilde{u}$, $\tilde{v}$, and $\tilde{w}$ for the three calibration curves, respectively.

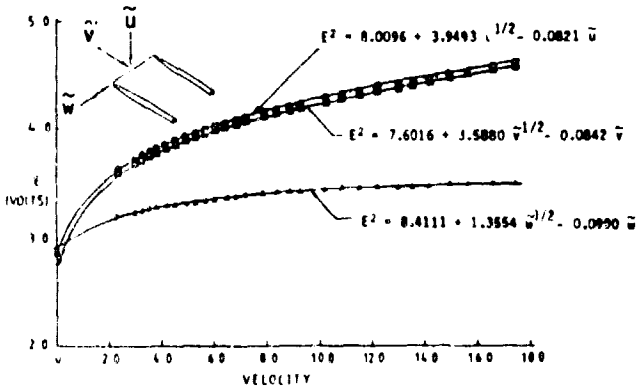

Figure 5. The Three-Directional Hot-Wire Calibration

When the wire is placed in a three dimensional flowfield, the effective cooling velocity experienced by the hot-wire is:

$$Z^2 = \tilde{v}^2 + G^2\tilde{u}^2 + K^2\tilde{w}^2 \qquad (2)$$

where G and K are the pitch and yaw factors defined by Jorgensen[17] to be:

$$G = \frac{\tilde{v}(\tilde{u} \text{ and } \tilde{w}=0)}{\tilde{u}(\tilde{v} \text{ and } \tilde{w}=0)}, \quad \text{and}$$

$$K = \frac{\tilde{v}(\tilde{u} \text{ and } \tilde{w}=0)}{\tilde{w}(\tilde{u} \text{ and } \tilde{v}=0)} \qquad (3)$$

which are evaluated from the three calibration curves (Figure 5) for a constant value of E^2. Equation (3) shows that the pitch and yaw factors are calculated with the $\tilde{v}$ component $i = 2$ in equation (1) of the effective cooling velocity as the reference. Therefore, the calibration constants used in equation (1) are the coefficients in the E vs. $\tilde{v}$ calibration of Figure 5., i.e., in a general flowfield:

$$E^2 = A_2 + B_2 Z^{1/2} + C_2 Z$$

with Z as given in Equation (2) above.

Figure 6 shows the pitch and yaw factors as a function of hot-wire voltage determined from the calibration curve of Figure 5. Both factors vary with hot-wire voltage, but the yaw factor is far more sensitive. The sensitivity analysis discussed in the next section demonstrates that uncertainties associated with the varying pitch and yaw factors do not seriously affect the accuracy of the estimated flow quantities.

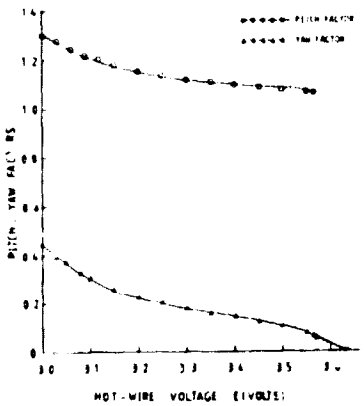

Figure 6. Pitch and Yaw Factors Plotted Against Hot-Wire Mean Effective Voltage

To carry out measurements in the confined jet flowfield, the wire is aligned in the flow in such a way that in the first orientation, the wire is normal to the flow in the axial direction and the probe coordinates coincide with the coordinates of

the experimental facility. Thus, the six equations for the instantaneous cooling velocities at the six orientations, as given by King[18] are:

$$
\begin{aligned}
Z_1^2 &= v^2 + G^2u^2 + K^2w^2 \\
Z_2^2 &= v^2 + G^2(u\cos 30^0 + w\sin 30^0)^2 \\
&\quad + K^2(w\cos 30^0 - u\sin 30^0)^2 \\
Z_3^2 &= v^2 + G^2(u\cos 60^0 + w\sin 60^0)^2 \\
&\quad + K^2(w\cos 60^0 - u\sin 60^0)^2 \\
Z_4^2 &= v^2 + G^2w^2 + k^2u^2 \qquad (4) \\
Z_5^2 &= v^2 + G^2(w\sin 120^0 + u\cos 120^0)^2 \\
&\quad + K^2(u\sin 120^0 - w\cos 120^0)^2 \\
Z_6^2 &= v^2 + G^2(w\sin 150^0 + u\cos 150^0)^2 \\
&\quad + K^2(u\sin 150^0 - w\cos 150^0)^2
\end{aligned}
$$

Solving simultaneously any three adjacent equations provide expressions for the instantaneous values of the three velocity components, u, w, and v in terms of the equivalent cooling velocities (Z_1, Z_2 and Z_3 for example, when the first three equations are chosen). Thus, the general form of the instantaneous velocity components is given as:

$$
\begin{aligned}
U &= \left[\left\{AO + \left(AO^2 + \frac{BO^2}{3}\right)^{1/2}\right\}\frac{1}{(G^2-K^2)}\right]^{1/2} \\
W &= \left[\left\{-AO + \left(AO^2 + \frac{BO^2}{3}\right)^{1/2}\right\}\frac{1}{(G^2-K^2)}\right]^{1/2} \qquad (5) \\
V &= \left[CO - \frac{(G^2+K^2)}{(G^2-K^2)}\left(AO^2 + \frac{BO^2}{3}\right)^{1/2}\right]^{1/2}
\end{aligned}
$$

The values of AO, BO and CO depend on the set of the three equations chosen and are given in Table 1 for appropriate equation sets.

TABLE 1

Values of AO, BO, and CO in Various Equation Sets

Equation Set P,Q,R Choice	AO	BO	CO
1, 2, 3	$(Z_2^2 - Z_1^2)$	$(-2Z_1^2 + 3Z_2^2 - Z_3^2)$	$(Z_1^2 - Z_2^2 + Z_3^2)$
2, 3, 4	$(Z_2^2 - Z_1^2)$	$(-Z_2^2 + 3Z_3^2 - 2Z_4^2)$	$(Z_2^2 - Z_3^2 + Z_4^2)$
3, 4, 5	$(Z_3^2 - 2Z_4^2 + Z_5^2)$	$(Z_3^2 - Z_5^2)$	$(Z_3^2 - Z_4^2 + Z_5^2)$
4, 5, 6	$(-Z_5^2 + Z_6^2)$	$(-2Z_4^2 + 3Z_5^2 - Z_6^2)$	$(Z_4^2 - Z_5^2 + Z_6^2)$
5, 6, 1	$(-Z_5^2 + Z_6^2)$	$(-Z_5^2 + 3Z_6^2 - 2Z_1^2)$	$(Z_5^2 - Z_6^2 + Z_1^2)$
6, 1, 2	$(-Z_6^2 + 2Z_1^2 - Z_2^2)$	$(-Z_6^2 + Z_2^2)$	$(Z_6^2 - Z_1^2 + Z_2^2)$

However, these equations cannot be directly used because it is impossible to obtain Z_1, Z_2 and Z_3 at a single instant in time with a single wire probe. Therefore, Equations (5) must be expressed in terms of mean and root-mean-square values. Equation (1) can be written as:

$$
Z_i = \left[-B_2 + \{B_2^2 + 4C_2(A_2 - E_i^2)\}^{1/2}/2C_2\right]^2 . \qquad (6)
$$

The above equation is in terms of instantaneous velocity Z_i and instantaneous voltage E_i. In order to obtain an expression for time-mean velocity as a function of time-mean voltage, a Taylor series expansion of Equation (6) can be carried out as follows:

$$
Z_i = Z_i(\bar{E}_i + E_i') = \phi(\bar{E}_i) + \frac{E_i'}{1!}\frac{\partial\phi}{\partial E_i} + \frac{E_i'^2}{2!}\frac{\partial^2\phi}{\partial E_i^2} + \cdots \qquad (7)
$$

where $\phi = Z_i(\bar{E}_i)$.

The Taylor series is truncated after second order terms assuming the higher order terms to be relatively small. Time averaging both sides of the above equation and employing the fact that $\overline{E'}=0$, yields:

$$
\bar{Z}_i = \phi + \frac{1}{2}\frac{\partial^2\phi}{\partial E_i^2}\sigma^2_{E_i} . \qquad (8)
$$

To obtain $\overline{Z_i'^2} = \sigma^2_{Z_i}$, the relationship as given by Hinze[19] is:

$$
\overline{Z_i'^2} = \sigma^2_{Z_i} = \text{Expec}\,[Z_i^2] - (\text{Expec}\,[Z_i])^2 . \qquad (9)
$$

Using Equation (8) as the basis, Expec $[Z_i^2]$ and $(\text{Expec}[Z_i])^2$ can be evaluated and substituted into Equation (8) to get:

$$
\overline{Z_i'^2} \simeq \sigma^2_{Z_i} = \frac{\partial\phi^2}{\partial E_i}\sigma^2_{E_i} - \left(\frac{1}{2}\frac{\partial^2\phi}{\partial E_i^2}\sigma^2_{E_i}\right)^2 \qquad (10)
$$

Thus, Equations (8) and (10) give the mean and variance of effective cooling velocities in terms of the mean and variance of the appropriate voltages.

In a 3-dimensional flow, it is usually desirable to obtain the mean and variance for the individual velocity components in axial, azimuthal, and radial directions, and also their cross correlations. The procedure to obtain the mean and variance of the individual velocity components is the same as for the effective cooling velocities except that u, w and v are functions of three random variables and there are extra terms in the Taylor expansion to account for the covariances of the cooling velocities. Thus, the axial mean velocity component as given by Dvorak and Syred,[16] and King[18] is:

$$
\bar{u} = U(\bar{Z}_P, \bar{Z}_Q, \bar{Z}_R) + \frac{1}{2}\sum_{i=1}^{3}\frac{\partial^2 U}{\partial Z_i^2}\sigma^2_{Z_i} + \sum_{i<j}^{3}\frac{\partial^2 U}{\partial Z_i \partial Z_j}K_{Z_iZ_j} \qquad (11)
$$

where $K_{Z_iZ_j}$ is the covariance of the cooling velocities Z_i and Z_j and is defined as:

$$K_{Z_iZ_j} = \frac{1}{T}\int_0^T (Z_i-\bar{Z}_i)(Z_j-\bar{Z}_j)\,dt \qquad (12)$$

Identical expressions for $\bar{w}$ and $\bar{v}$ can also be obtained in terms of W and V, respectively. Derivatives of the form $\partial^2U/\partial Z_i\partial Z_j$ are determined analytically from equations (5) and Table 1.

Also, the normal stresses are given as:

$$\overline{u'^2} = \sum_{i=1}^{3}\left(\frac{\partial U}{\partial Z_i}\right)^2 \cdot \sigma_{Z_i}^2 + \sum_{i\neq j}^{3}\sum_{j}^{3}\frac{\partial U}{\partial Z_i}\cdot\frac{\partial U}{\partial Z_j}\cdot K_{Z_iZ_j}$$

$$-\left[\frac{1}{2}\sum_{i=1}^{3}\frac{\partial^2 U}{\partial Z_i^2}\cdot\sigma_{Z_i}^2 + \sum_{i<j}^{3}\frac{\partial^2 U}{\partial Z_i\partial Z_j}\cdot K_{Z_iZ_j}\right]^2 \qquad (13)$$

with similar expressions for $\overline{w'^2}$ and $\overline{v'^2}$.

Finally, the expressions for shear stresses as given by Dvorak and Syred[16] are of the form:

$$\overline{u'v'} = \sum_{i=1}^{3}\frac{\partial U}{\partial Z_i}\frac{\partial V}{\partial Z_i}\sigma_{Z_i}^2 + \sum_{i\neq j}^{3}\sum_{j}^{3}\frac{\partial U}{\partial Z_i}\frac{\partial V}{\partial Z_j}K_{Z_iZ_j}$$

$$-\left[\frac{1}{2}\sum_{i=1}^{3}\frac{\partial^2 U}{\partial Z_i^2}\sigma_{Z_i}^2 + \sum_{i<j}^{3}\sum_{j}^{3}\frac{\partial^2 U}{\partial Z_i\partial Z_j}\cdot K_{Z_iZ_j}\right]$$

$$\cdot\left[\frac{1}{2}\sum_{i=1}^{3}\frac{\partial^2 V}{\partial Z_i^2}\cdot\sigma_{Z_i}^2 + \sum_{i<j}^{3}\sum_{j}^{3}\frac{\partial^2 V}{\partial Z_i\partial Z_j}\cdot K_{Z_iZ_j}\right] \qquad (14)$$

Expressions for $\overline{u'w'}$ and $\overline{v'w'}$ can also be obtained in a similar manner and are given in Reference 22.

3.2 Calculation of Covariances

Dvorak and Syred[16] used a DISA time correlator (55A06) to find the correlation coefficients between the velocity fluctuations in the three directions. King's approach is to use the information obtained by all six orientations and devise a mathematical procedure to calculate the covariances.

Covariances are calculated using the relationship:

$$K_{Z_iZ_j} = \gamma_{Z_iZ_j}\left[\sigma_{Z_i}^2\ \sigma_{Z_j}^2\right]^{1/2} \qquad (15)$$

where $\gamma_{Z_iZ_j}$ is the correlation coefficient between the two cooling velocities Z_i and Z_j. By definition, the absolute value of the correlation coefficient $\gamma_{Z_iZ_j}$ is always less than 1.

King[18] made certain assumptions to calculate the covariances. However, he observed that at times the calculated value of the correlation coefficient is greater than one at which instance he assigned previously fixed values to the correlation coefficients. He argued that if two wires are separated by an angle of 30 degrees, the fluctuating signals from the wires at the two locations would be such that their contribution to the cooling of the wire would be related by the cosine of the angle between the wires. This assumption leads to the following three values of the correlation coefficients.

$$\gamma_{Z_PZ_Q} = \cos 30 = 0.9$$
$$\gamma_{Z_QZ_R} = \cos 30 = 0.9 \qquad (16)$$

To relate $\gamma_{Z_PZ_R}$ with $\gamma_{Z_PZ_Q}$ and $\gamma_{Z_QZ_R}$, King introduced the following relationship:

$$\gamma_{Z_PZ_R} = \eta\,\gamma_{Z_PZ_Q}\,\gamma_{Z_QZ_R} \qquad (17)$$

where η is given a value of 0.8. Hence $\gamma_{Z_PZ_R}$ becomes:

$$\gamma_{Z_PZ_R} = (0.8)(0.9)(0.9) = 0.65 \qquad (18)$$

The three covariances are then obtained by substituting the corresponding values of the correlation coefficients into Equation (15).

The present study, however, uses Equations (16) and (18) during the entire data reduction. The reason for this is contained in the results of the sensitivity analysis presented in the next section. This analysis demonstrated that there is not significant error magnification in the data reduction due to the correlation terms.

4. Results of Hot-Wire Measurements

The six-orientation hot-wire technique was employed to measure the turbulence quantities for swirling and non-swirling flow conditions in the confined jet facility described earlier. Also, an extensive sensitivity analysis of the data reduction was conducted to assist the estimation of the uncertainties in the output quantities.

4.1 Uncertainty Analysis

The uncertainty analysis includes a determination of the sensitivity of the six-orientation hot-wire data reduction to various input parameters which have major contributions in the response equations. Pitch and yaw factors (G and K) are used in the response equations described in Section 3 in order to account for the directional sensitivity of the single hot-wire probe. Figure 6 shows the pitch and the yaw factors plotted against the hot-wire mean effective voltage. Both the pitch and yaw factors are functions of the hot-wire mean effective voltage, but the yaw factor is far more sensitive. A one percent increase in the hot-wire voltage reduces the pitch factor by 1.3 percent and the yaw factor by 56 percent. For the present study, the values of these factors are chosen at an average hot-wire voltage experienced in the flowfield. This was appropriate since the output quantities ($\bar{u}$, u'_{rms}, $\overline{u'v'}$, etc) are only weakly dependent on the value of K. This can be seen in the data of Table 2 which summarizes a sensitivity analysis performed on the data reduction program at a

representative position in the flowfield.

Table 2 demonstrates the percent change in the output quantities for a 1 percent change in most of the important input quantities. For the data presented in this table only quantities calculated from the probe orientation combination $\bar{Z}_5$, $\bar{Z}_6$ and $\bar{Z}_1$ are used, for simplicity. In this swirling flow $\bar{Z}_6$ was the minimum of the 6 mean effective cooling velocities. King[18] has argued that the probe orientation combination approximately centered around the minimum effective cooling velocity produces more accurate estimates of calculated turbulence quantities, than do the other orientation combinations.

TABLE 2

Effect of Input Parameters on Turbulence Quantities

PARAMETER	% CHANGE IN PARAMETER	% CHANGE IN TIME-MEAN AND TURBULENCE QUANTITIES								
		$\bar{u}$	$\bar{v}$	$\bar{w}$	u'_{rms}	v'_{rms}	w'_{rms}	$\overline{u'v'}$	$\overline{u'w'}$	$\overline{v'w'}$
$\bar{Z}_1$	+1	+16.10	+0.66	+4.98	+15.75	-2.06	+2.75	+6.0	+51.43	+11.94
$\bar{Z}_5$	+1	+2.19	-2.21	+11.49	-6.50	+2.42	+12.88	+4.0	+14.29	+7.46
$\bar{Z}_6$	+1	-10.59	-0.36	-8.50	-1.88	+7.07	-9.54	-6.0	-54.29	-11.94
$\bar{Z}_{1_{rms}}$	+1	+0.27	-0.06	+0.14	+1.63	+0.13	+0.39	+2.0	+2.86	+1.49
$\bar{Z}_{5_{rms}}$	+1	+0.05	0.0	+0.14	0.0	-0.13	+1.57	0.0	0.0	+1.49
$\bar{Z}_{6_{rms}}$	+1	-0.16	+0.18	-0.14	-0.63	+1.03	-1.08	-2.0	-5.71	0.0
γ	+1	-1.02	0.0	-1.01	-1.0	0.0	-0.98	-2.0	-2.86	-1.49
κ	+1	+0.01	-0.04	+0.01	+0.01	0.0	-0.01	0.0	0.0	0.0
$\bar{Z}_5\bar{Z}_6$	+1	+0.05	0.0	+0.14	-0.13	-0.13	-1.77	0.0	-2.86	+1.49
$\bar{Z}_6\bar{Z}_R$	+1	+0.21	+0.01	+0.05	-1.63	+0.13	-0.39	0.0	-5.71	+1.49
$\bar{Z}_6\bar{Z}_\theta$	+1	-0.16	+0.18	-0.09	+0.13	0.0	+0.69	-2.0	+2.86	0.0

It is not unusual in hot-wire anemometry to have the mean velocity components and turbulence quantities that are measured, be quite sensitive to changes in mean hot-wire voltage. For interpretive purposes, the mean hot-wire voltage variations can be thought of as being either errors in measuring the mean voltage, or shifts in the individual wire calibrations due to contamination or strain 'aging' of the wire. The data of Table 2 demonstrate that the most serious inaccuracies in the measurement and data reduction technique will be in the estimates of turbulent shear stresses, the most inaccurate output term being $\overline{u'w'}$.

As already discussed in Section 3, an *ad hoc* assumption is made regarding the numerical values of the correlation coefficients used in the deduction of time-mean and turbulence quantities. The results of the sensitivity analysis (Table 2) show the time-mean and turbulence quantities to be relatively insensitive to variations in the correlation coefficients. Therefore, the major *ad hoc* assumption made in the technique does not seem to have a great effect on the output quantities compared to the effect of other input quantities.

As mentioned earlier, turbulence quantities (the output) can be calculated from six combinations of data from adjacent wire orientations. One measure of the uncertainty in the output quantities can be obtained by examining the variance in these quantities calculated from the six different position combinations. Table 3 shows these comparison data for a representative position in the flowfield.* For each of the output quantities, an ensemble mean $\bar{x}$ is calculated together with an ensemble standard deviation σ. The ratio σ/x is a measure of the uncertainty in the output quantity. In this table, NR stands for 'not resolved', a problem that occurs when the data reduction program attempts to take the square root of a negative quantity. In addition, quantities which are more than three standard deviations outside the mean are rejected as spurious calculations.

TABLE 3

Scatter Among the Turbulence Quantities When Solved by Six Different Combinations

TURBULENCE QUANTITY	TURBULENCE QUANTITY SOLVED BY SIX COMBINATIONS						MEAN $\bar{x}$	STANDARD DEVIATION σ	$\sigma/\bar{x}$
	1,2,3	2,3,4	3,4,5	4,5,6	5,6,1	6,1,2			
$\bar{u}/\bar{u}_o$	0.21	0.20	0.21	0.21	0.19	0.18	0.20	0.01	0.06
$\bar{v}/\bar{u}_o$	0.10	NR*	0.11	0.17	0.17	0.17	0.14	0.04	0.26
$\bar{w}/\bar{u}_o$	0.40	0.39	0.39	0.38	0.37	0.40	0.39	0.01	0.03
$u'_{rms}/\bar{u}_o$	0.14	0.14	0.14	0.07	0.08	0.08	0.11	0.03	0.31
$v'_{rms}/\bar{u}_o$	0.06	0.11	0.11	0.08	0.08	0.09	0.09	0.02	0.23
$w'_{rms}/\bar{u}_o$	0.13	0.16	0.10	0.11	0.10	0.12	0.12	0.02	0.20
$\overline{u'v'}/\bar{u}_o^2$	NR*	NR*	0.012	NR*	0.005	0.004	0.007	0.004	0.62
$\overline{u'w'}/\bar{u}_o^2$	0.002	0.010	0.002	0.004	0.004	0.008	0.005	0.003	0.72
$\overline{v'w'}/\bar{u}_o^2$	0.003	NR*	0.003	0.003	0.007	0.001	0.003	0.002	0.58

* Not Resolved

The data in Tables 2 and 3 can be used to produce estimates in the uncertainties of the calculated turbulence quantities. The data suggest that uncertainties on the order of 5 percent are to be expected in the mean velocity component estimates. Normal turbulent stress estimates (u'_{rms}, etc.) have uncertainties on the order of 20 to 30 percent and turbulent shear stress estimates are significantly higher, although most of this is a consequence of taking a product of terms such as u' and v'.

These uncertainty estimates are considered to be somewhat conservative. More accurate estimates are quite difficult to obtain because, to our knowledge, similar measurements have not been performed with any other instrumentation system in this geometry flowfield. Also, comparisons of several representative points with independent measurements suggest that the ensemble averages estimates are typically in closer agreement than are selected sets of three orientations. Therefore, all turbulence estimates presented in this paper are calculated from ensemble averages of six groups of three adjacent wire orientations. Any data not resolved are not included in this averaging. This approach represents a departure from the technique developed by King[18] who typically

* x/D=1.5, r/D=0.25, ϕ=38 deg (swirling flow).

selected one group of three orientations from which to calculate his turbulence estimates.

4.2 Results of Flowfield Surveys

Radial distributions of time-mean velocities, turbulent normal stresses and shear stresses are obtained for both nonswirling and swirling conditions, at various axial locations in the flowfield.

Nonswirling Flow. In the confined jet, the experiments have been conducted with expansion angles of 90 degrees (sudden expansion) and 45 degrees (gradual expansion) and the results for both cases are presented in Reference 22. In the interest of brevity, only the data for a 90 degree expansion are presented here.

Figure 7 shows the radial distribution of time-mean axial and radial velocity components at various axial locations. The axial velocity distributions are compared with a similar study performed by Chaturvedi[5] with a crossed hot-wire probe. Because of the inability of the six-orientation hot-wire technique to determine the sense of the flow direction in a nonswirling flow, the presence of the corner recirculation zone was observed by a sudden increase in the axial velocity closer to the wall.

Figure 8 shows the radial distribution of axial and radial components of the turbulence intensity at various axial locations in the confined jet flowfield. These turbulence intensity components are compared with Chaturvedi's measurements[5] and reasonable agreement is found. In fact, the agreement in most cases is better than the uncertainty estimates derived from the data reduction sensitivity analysis.

Included on Figure 8 are measured turbulent shear stress component ($\overline{u'v'}/U_0^2$) profiles for the nonswirling confined jet. For the most part, these measurements are in reasonable agreement with those made by Chaturvedi[5] with a crossed wire probe. The two significant exceptions to the good agreement occur at the furthest upstream and furthest downstream locations. Upstream, at x/D = 0.5 the shear layer is very thin and, therefore, matching data from several wire orientations obtained at somewhat different times may be practically difficult. We believe the overly large measured turbulent shear stress on the centerline at the furthest downstream station (x/D = 3.0) to be a consequence of the transient nature of the flow. The recirculation regions in the confined jet oscillate somewhat at a low frequency, likely characteristic of the main acoustic modes in the tube. These large scale oscillations can have significant correlated velocity fluctuations (such as $\overline{u'v'}$).

Swirling Flow The measurements performed in the swirling flow are with α = 90°, Φ = 38°, and x/D = 0.5, 1.0, and 1.5. The object of these limited number of experiments was to evaluate the reliability and accuracy of the six-orientation hot-wire technique before making extensive use of the technique.

The hot-wire results in the case of time-mean axial and azimuthal (swirl) velocities shown in Figures 9 and 10, are compared with five-hole pitot probe measurements performed by Rhode[3] in the same experimental facility. Agreement among the two studies is fairly good. King[18] suggested a method to determine the sense of the axial velocity. He advised comparing the magnitudes of Z_3 and Z_5 given by Equations 4. In the present flowfield, the swirl velocity is always positive and the two equations giving Z_3 and Z_5 differ only in the sign of axial velocity. Therefore, when Z_5 is greater than Z_3, the axial velocity is negative, otherwise it is positive. With the proper sense being assigned to the x velocity mean component, the presence of central toriodal recirculation zone is evident in the results of both measurement techniques.

Figure 11 shows the radial distribution of the time-mean radial velocity at various axial locations for a swirl vane angle of 38 degrees and wall expansion angle of 90 degrees. Flow visualization and five-hole pitot probe measurements performed in Rhode's study[3] show the time-mean radial velocity to be negative at axial locations greater than x/D = 0.5. In spite of the inability of the six-orientation hot-wire technique to determine the sense of the radial velocity, the data are presented with the appropriate sign change. There is a reasonable agreement among the two studies in measurements of time mean radial velocities except at the initial measurement station.

Figure 12 shows the radial distribution of axial, radial and azimuthal turbulent intensities at three axial locations presented. At axial locations closer to the inlet of the confined jet, the axial turbulence intensity is fairly high, up to 32 percent for x/D = 0.5 which is due to the large axial velocity gradients closer to the wall. However, in the case of radial turbulence intensity, the profiles are rather flat. The mean azimuthal velocity also experiences sudden changes in gradients and, hence, the outcome is a large azimuthal turbulence intensity closer to the wall at x/D = 0.5.

Figure 13 shows the shear stresses $\overline{u'v'}/U_0^2$, $\overline{u'w'}/U_0^2$, and $\overline{v'w'}/U_0^2$ as a function of radial and axial distance. The sensitivity analysis showed that we should expect large uncertainties associated with evaluation of turbulent shear stresses using the six-orientation technique. Therefore, the reliability of the profiles of these shear stresses shown in Figure 13 is uncertain at this time. Nevertheless, stresses $\overline{u'v'}/U_0^2$ and $\overline{u'w'}/U_0^2$ are found to have large values closer to the wall that one would expect due to steep axial and azimuthal velocity gradients. The fact that we have found no other measurements of this type in a swirling, recirculating flow attests to the fact that accurate measurements in such a flow are quite difficult.

Closure

The six-orientation hot-wire technique is a relatively new method to measure time-mean velocity components and turbulence quantities in complex three-dimensional flowfields. Applied in

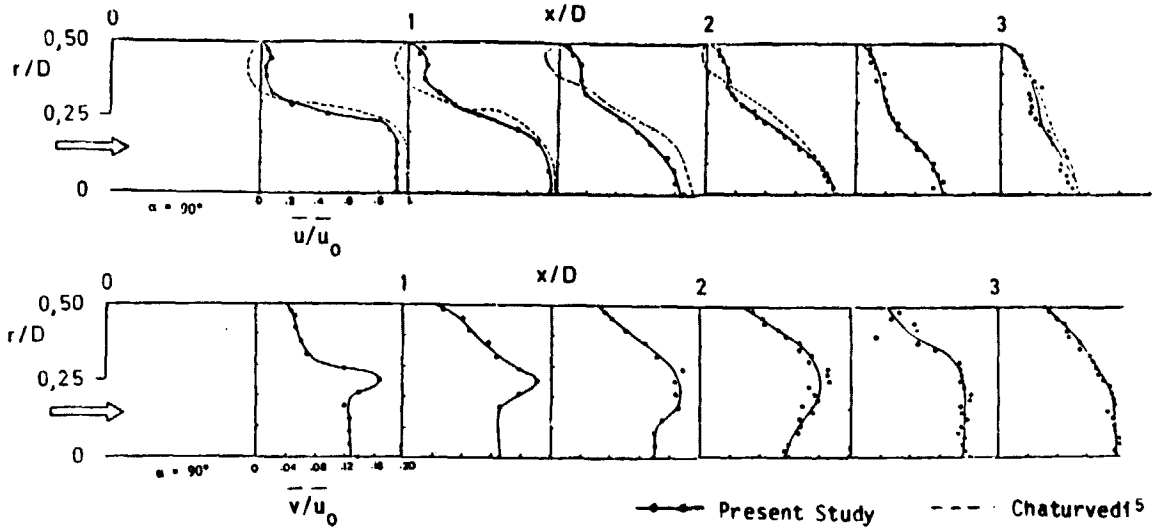

Figure 7. Radial Distributions of Time-Mean Axial and Radial Velocity Components in the Non-Swirling Confined Jet; (Note the Difference in Velocity Scales)

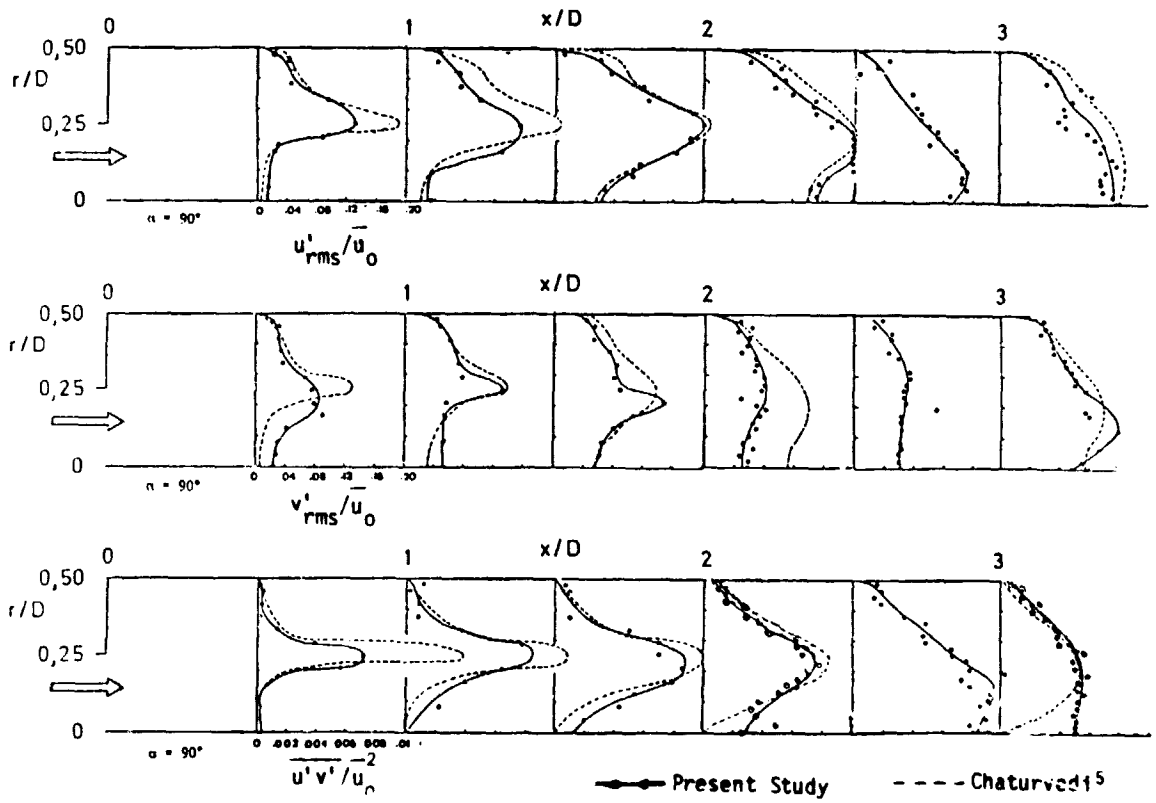

Figure 8. Radial Distributions of Turbulent Intensities $u'_{rms}/\overline{u}_0$, $v'_{rms}/\overline{u}_0$ and shear stress $\overline{u'v'}/u_0^2$

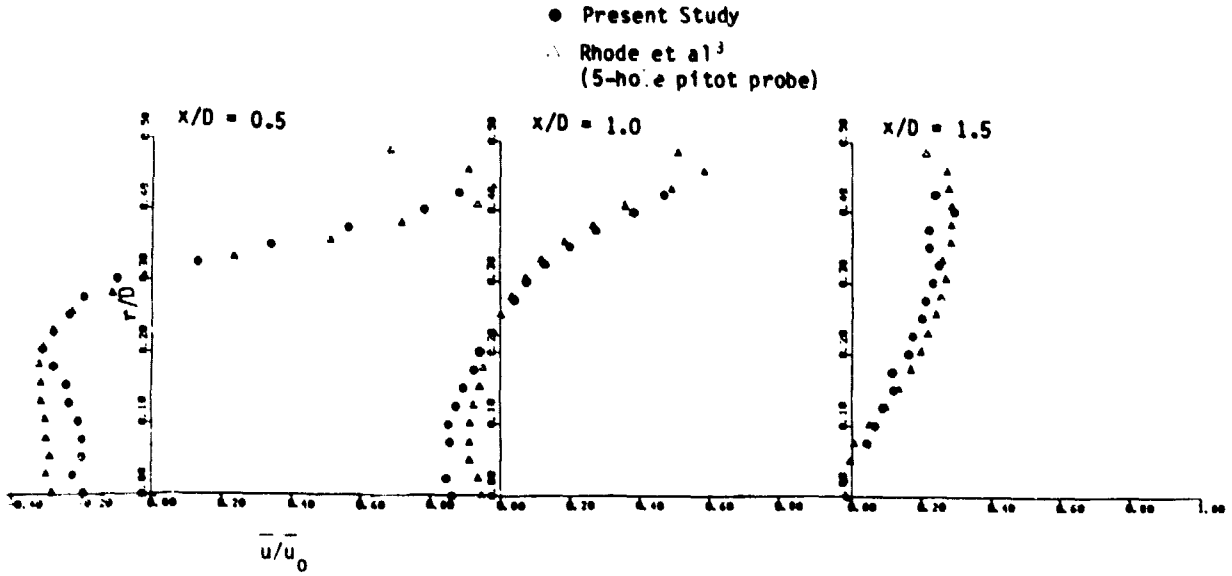

Figure 9. Radial Distribution of Time-Mean Axial Velocity in Swirling Confined Jet for $\alpha = 90°$ and $\Phi = 38°$

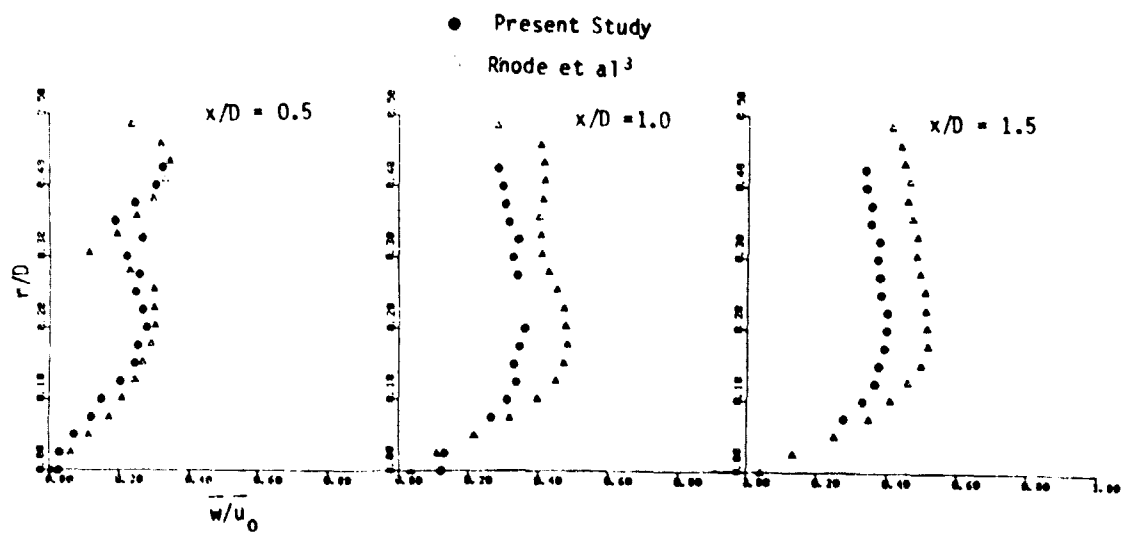

Figure 10. Radial Distribution of Time-Mean Azimuthal Velocity in Swirling Confined Jet for $\alpha = 90°$ and $\Phi = 38°$

this study to nonreacting axisymmetric flowfields, measurements of time-mean and root-mean-square voltages at six different orientations contain enough information to obtain the time-mean velocities, turbulence intensities and shear stresses. At each location in the flow, there are six different values of each of the above quantities that can be obtained using six sets of measurements of three adjacent orientations. Ensemble averages of the output quantities from the six combinations of data appear to produce estimates with the best agreement with independent measurements.

Flowfield surveys of both swirling and non-swirling confined jets have been made with the six-orientation single hot-wire technique. These measurements have been used to calculate estimates of the mean velocity components and the normal and shear turbulent stresses. Where independent data exist, comparisons have been made which demonstrate the reliability of the technique.

In addition, a sensitivity analysis of the data reduction technique has been conducted which

forms the major ingredient in the uncertainty analysis. It is demonstrated that the largest uncertainties are to be expected in the turbulent shear stress estimates. Nevertheless, in non-swirling flows the measured shear stresses are in reasonable agreement with previous measurements made with a crossed-wire probe. In swirling flow, previous similar measurements have not been found. Consequently, the universal accuracy of the measured technique applied to swirl flows is still an open question.

Acknowledgement

The authors wish to extend their sincere gratitude to NASA Lewis Research Center and the Air Force Wright Aeronautical Laboratories for support under Grant No. NAG3-74.

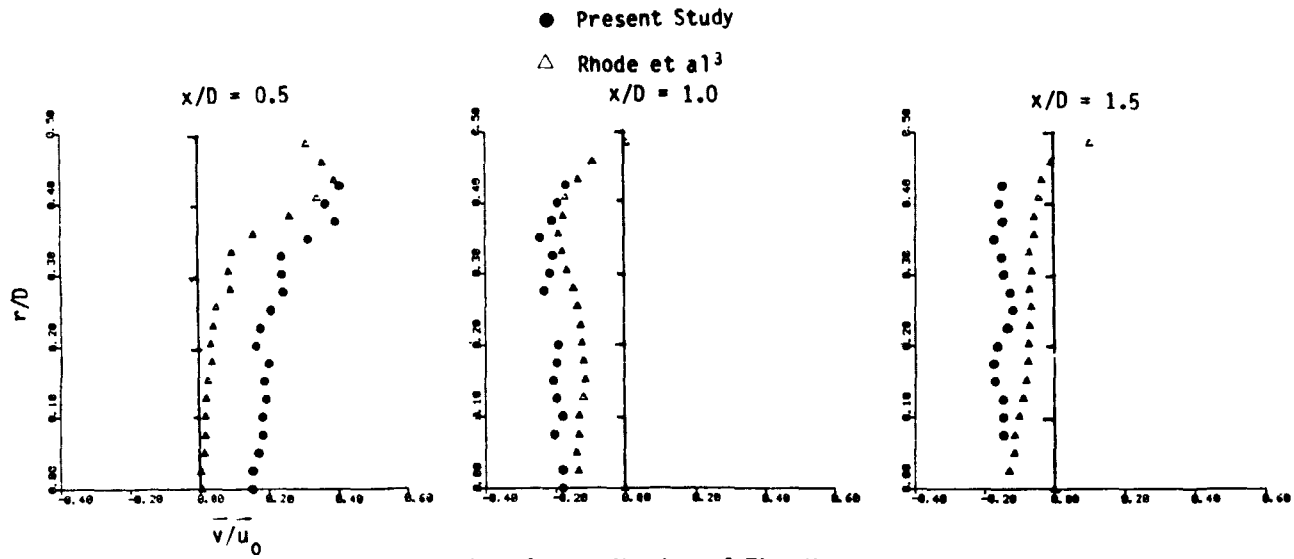

Figure 11. Radial Distribution of Time-Mean Radial Velocity in Swirling Confined Jet for $\alpha = 90°$ and $\Phi = 38°$

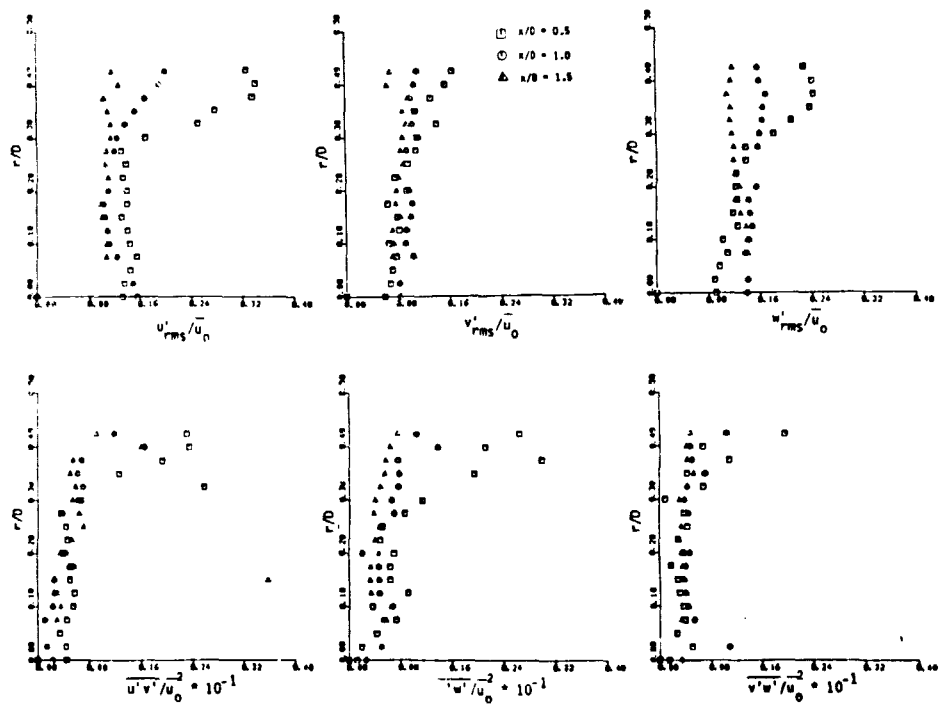

Figure 12. Radial Distribution of Turbulent Shear Stresses $\overline{u'v'}/u_0^2$, $\overline{u'w'}/u_0^2$, and $\overline{v'w'}/u_0^2$ in Swirling Confined Jet for $\alpha = 90°$ and $\Phi = 38°$

References

1 Lilley, D.G., "Flowfield Modeling in Practical Combustors: A Review," Journal of Energy, 3, No. 4, 1979.

2 Lilley, D.G. and Rhode, D.L., "A Computer Code for Swirling Turbulent Axisymmetric Recirculating Flows in Practical Isothermal Combustor Geometries," NASA Contractor Report 3442, February 1982.

3 Rhode, D.L., Lilley, D.G. and McLaughlin, D.K., "Mean Flowfields in Axisymmetric Combustor Geometries with Swirl," AIAA Paper No. 82-0177, 1982, AIAA Journal (in press).

4 Krall, K.M. and Sparrow, E.M., "Turbulent Heat Transfer in the Separated, Reattached, and Redevelopment Regions of a Circular Tube," Journal of Heat Transfer, pp. 131-136, February 1966.

5 Chaturvedi, M.C., "Flow Characteristics of Axisymmetric Expansions," Proceedings, Journal of the Hydraulic Division, ASCE, 89, No. HY3, pp. 61-92, 1963.

6 Phaneuf, J.T. and Netzer, D.W., Flow Characteristics in Solid Fuel Ramjets, Report No. NPS-57Nt74081. Prepared for the Naval Weapons Center by the Naval Postgraduate School, Monterey, California, July 1974.

7 Back, L.H. and Roschke, E.J., "Shear Layer Flow Regimes and Wave Instabilities and Reattachment Lengths Downstream of an Abrupt Circular Channel Expansion," Journal of Applied Mechanics pp. 677-681, September 1972.

8 Roschke, E.J. and Back, L.H., "The Influence of Upstream Conditions on Flow Reattachment Lengths Downstream of an Abrupt Circular Channel Expansion," Journal of Biomechanics, 9, pp. 481-483, 1976.

9 Ha Minh, H. and Chassaing, P., "Perturbations of Turbulent Pipe Flow," Proceedings, Symposium on Turbulent Shear Flows. Pennsylvania State University, pp. 13.9-13.17, April 1977.

10 Moon, L.F. and Rudinger, G., "Velocity Distribution in an Abruptly Expanding Circular Duct," Journal of Fluids Engineering, pp. 226-230, March 1977.

11 Bradshaw, P., An Introduction to Turbulence and Its Measurement, Pegamon Press, New York, 1971.

12 Beer, J.M. and Chigier, N.A. Combustion Aerodynamics, Halsted Press Division, John Wiley & Sons, Inc., New York, 1972.

13 Syred, N., Beer, J.M. and Chigier, N.A., "Turbulence Measurements in Swirling Recirculating Flows," Proceedings, Salford Symposium on Internal Flows, London, England: Inst. of Mechanical Engineering, pp. 827-836, 1971.

14 Wygnanski, I, and Fiedler, H., "Some Measurements in the Self Preserving Jet," Journal of Fluid Mechanics, 38, p. 577, 1969.

15 Pratte, B.D. and Keffer, J.R., "The Swirling Turbulent Jet," Journal of Basic Engineering, 94, pp. 739-748, December 1972.

16 Dvorak, K. and Syred, N., "The Statistical Analysis of Hot Wire Anemometer Signals in Complex Flow Fields," DISA Conference, University of Leicester, 1972.

17 Jorgensen, F.E., "Directional Sensitivity of Wire and Fiber Film Probes," DISA Information No. 11, Franklin Lakes, N.J., pp. 31-37, May 1971.

18 King, C.F., "Some Studies of Vortex Devices - Vortex Amplifier Performance Behavior," Ph.D. Thesis, University College of Wales, Cardiff, Wales, 1978.

19 Hinze, J.O. Turbulence, 2nd Edition, McGraw-Hill, New York, 1975.

20 Habib, M.A. and Whitelaw, J.H., "Velocity Characteristics of Confined Coaxial Jets With and Without Swirl," ASME Paper 797-WA/FE-21, New York, N.Y., December 2-7, 1979.

21 Gupta, A.K. and Lilley, D.G., Flowfield Modeling and Diagnostics, Abacus Press, Tunbridge Wells, England, 1982 (in press).

22 Janjua, S.I., "Turbulence Measurements in a Complex Flowfield Using a Six-Orientation Hot-Wire Probe Technique," M.S. Thesis, Oklahoma State University, Stillwater, Oklahoma, December 1981.